LEMoN: Label Error Detection using Multimodal Neighbors

Haoran Zhang* **Aparna Balagopalan*** **Nassim Oufattole** **Hyewon Jeong**
Yan Wu **Jiacheng Zhu** **Marzyeh Ghassemi**
Massachusetts Institute of Technology
{haoranz, aparnab}@mit.edu

Abstract

Large repositories of image-caption pairs are essential for the development of vision-language models. However, these datasets are often extracted from noisy data scraped from the web, and contain many mislabeled examples. In order to improve the reliability of downstream models, it is important to identify and filter images with incorrect captions. However, beyond filtering based on image-caption embedding similarity, no prior works have proposed other methods to filter noisy multimodal data, or concretely assessed the impact of noisy captioning data on downstream training. In this work, we propose LEMoN, a method to automatically identify label errors in multimodal datasets. Our method leverages the multimodal neighborhood of image-caption pairs in the latent space of contrastively pretrained multimodal models. We find that our method outperforms the baselines in label error identification, and that training on datasets filtered using our method improves downstream classification and captioning performance.

1 Introduction

Machine learning datasets used to train and finetune large vision, language, and vision-language models frequently contain millions of labeled instances [64, 35, 73, 7]. Prior work highlights that some instances in such datasets may be mislabeled [54, 47, 39, 5, 58], as seen in Figure 1. This is especially problematic in settings such as healthcare, where the reliability of downstream models may depend on the quality of data used for pretraining [9, 43, 45].

Identifying and correcting label errors in existing datasets at scale would lead to more reliable and accurate models in the real world [82, 71, 39, 5]. However, given the large size of such datasets, manual detection of errors is practically infeasible. This is evidenced by the growth of models trained on noisy data with the web [35, 73, 44], or with model generated pseudo-labels [48, 33].

Machine learning (ML) based approaches to automatically identifying label errors have also been proposed in prior work [57, 67, 37, 2, 82, 53]. However, we identify two critical limitations: (1) a majority of such works are *unimodal*: i.e., they only utilize image-based representations and detection strategies, and (2) many of the best-performing approaches depend on having access to a model already trained on the downstream tasks of interest [57, 67]. We hypothesize that applying a neighborhood-based approach to multimodal representations in the form of image-text pairs can improve label error detection without requiring task-specific training, which may be costly and/or domain specific for some datasets.

Figure 1: Samples from classification and captioning datasets discovered to be mislabeled by our method.

*Equal contribution.

Workshop on Responsibly Building the Next Generation of Multimodal Foundational Models
38th Conference on Neural Information Processing Systems (NeurIPS 2024).

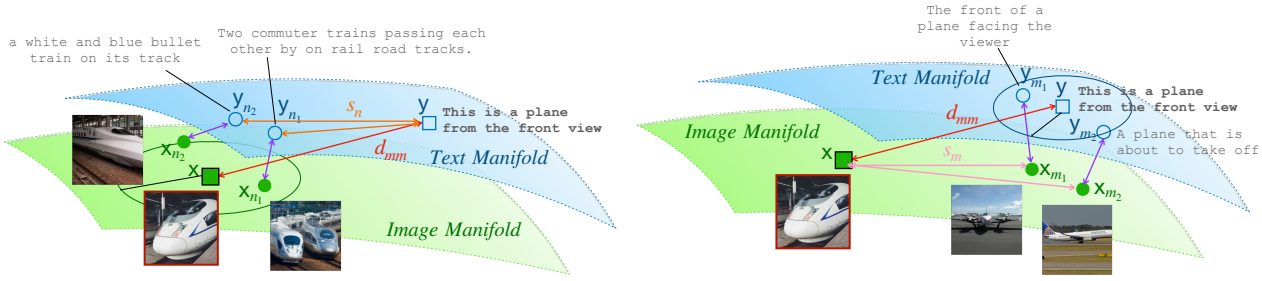

(a) (b)

Figure 2: **Outline of LEMoN**, our proposed method for multimodal label error detection. We demonstrate LEMoN on a real sample from the MSCOCO dataset, where an image of a train ($\mathbf{x}$) is mislabeled as $\mathbf{y}$ = "`This is a plane from the front view`". (a) We compute the simple CLIP similarity $d_{mm}(\mathbf{x}, \mathbf{y})$. We then find the nearest neighbors of $\mathbf{x}$ in the image space ($\mathbf{x}_{n_j}$) and compute the distance between the corresponding texts and $\mathbf{y}$ to compute the score component s_n. (b) To compute the score component s_m, we find the nearest neighbors of $\mathbf{y}$ in the text space ($\mathbf{y}_{m_k}$), and compute the distance between the corresponding images and $\mathbf{x}$.

Additionally, a common assumption made in prior works is that each label is one-of-k classes [2, 82]. The vast majority of label error detection methods proposed in prior works are hence for *classification* datasets. In contrast, datasets used to train large vision-language models contain natural language labels such as image captions [35, 34, 73]. Methods to filter out instances with noisy labels – e.g., based on the similarity of image and caption representations – have been utilized in prior work with some success [35, 30] for such datasets. However, to the best of our knowledge, no prior works have proposed or rigorously compared methods to identify errors in datasets with natural language labels, or assessed the impact of detection on downstream tasks like image captioning.

In this work, we propose LEMoN– **L**abel **E**rror detection using **M**ultim**o**dal **N**eighbors – a method for multimodal label error detection, which can be applied to image-text pairs in datasets such as MSCOCO [42]. While prior techniques utilize unimodal neighbors for label error detection, LEMoN leverages multi-modal neighborhoods derived using contrastively pretrained vision-language models such as Contrastive Language-Image Pretraining (CLIP) [59]. Specifically, in addition to considering pairwise image-text distances, we also retrieve nearest neighbors in the image and text space as illustrated in Figure 2. This is motivated about rich neighborhood geometry in the joint embedding space of multimodal models [38, 62]. We then compute distance scores with neighbors in each modality and combine these into a single score measuring the likelihood of a label error, with the intuition that higher discordance (or higher distance) with neighbors indicates a higher chance of label error. We validate the utility of these scores across eight datasets, including one in a healthcare setting, and compare to over ten baselines.

Our key contributions and findings are as follows:

- We propose LEMoN, a novel, theoretically justified multimodal method capable of detecting label errors in large image-caption datasets (Section 3).
- We show that LEMoN outperforms all downstream task-unaware baselines for label error detection in the classification setting, by up to 3.4% AUROC (Section 6.1).
- We empirically show that LEMoN outperforms baselines in three out of four captioning datasets, by up to 3.9% AUROC (Section 6.1).
- We demonstrate that LEMoN improves performance on downstream classification and captioning models by filtering out data predicted to be label errors. (Section 6.2).
- Finally, we verify that the predictions generated by LEMoN are meaningful through a real world analysis of LEMoN on existing datasets without known label errors (Section 6.4).

2 Related Works

Label Noise Detection Noisy and incorrect labels [5] in training data may lead to decreased or "destabilized" [53, 47] performance on downstream tasks [8, 54]. Two orthogonal approaches can be taken to reduce the adverse effects of such labels: developing methods to learn in the presence of label errors [11, 51, 27], and/or detecting and filtering out instances with label errors [21]. In this work, we focus on the latter approach. Prior approaches [67, 2, 57, 53, 37, 76, 32] for automatic label error detection include relying on the training dynamics of task-specific downstream models [67]

and neighborhood-based strategies [2, 21]. Some of these techniques are fully supervised [53, 8] or unsupervised [57, 67, 21, 2], use pre-trained generative models [17] or are fully training-free approaches [82, 37]. Previous approaches for label error detection closest to this work includes deep k-nearest neighbor (deep k-NN) methods using k-NN entropy on vector space embeddings [2, 21] and SimiFeat [82] which employs a local neighborhood-based voting or ranking for noise identification. In contrast to these methods, our work enhances label noise detection by harnessing information across *multiple data modalities*, such as image and text. Finally, though prior works may have utilized the idea of semantic neighborhoods in multimodal data (e.g. for cross-modal retrieval) [68, 69], we believe we are the first to extend concepts to the task of label error detection by proposing a novel, theoretically justified score for identifying label errors.

Contrastive Learning Contrastive learning is a representation learning strategy that contrasts positive and negative pairs of data instances [10, 49, 3] to learn an embedding space. The core idea is to embed similar data points (positive pairs) closer together than dissimilar data points (negative pairs) [63, 66, 55]. In this work, we primarily utilize pre-trained models that use the CLIP loss (where the pre-training objective is predicting which text caption goes is paired with which image) for jointly embedding image and text data [59].

Image Captioning The goal of image captioning is to describe a given image [15] in natural language. Prior approaches for caption generation have included supervised training of end-to-end models from scratch [74, 41, 25, 77, 15]. More recently, vision-language models pretrained on large datasets of noisy image-caption pairs extracted from the web [35, 34, 73] – such as CC12M [7] – have been utilized for captioning. Some of the pretraining tasks include image-text contrastive learning, image-text matching, and/or retrieval [35], as well as general purpose text generation conditioned on an input image [73]. Given that datasets for training such large models are noisy [30], several steps have been utilized in prior work to filter out noisy captions during training. The most common strategy involves computing the similarity between representations of the image and caption text using another pretrained model (e.g., CLIP) prior to training [30]. Another approach in training the BLIP [35] model is to synthetically generate noisy captions and train a classifier to distinguish between high quality captions and noisy captions with a cross-entropy loss [35]. To the best of our knowledge, no previous work has conducted a comprehensive comparison of various strategies for label error detection in captioning datasets.

Multimodal Neighborhood Methods Previous studies [36, 68, 69, 26, 38, 6] have examined the geometry of neighborhood spaces in multimodal models, often with the goal of improving representation learning [26, 36] or retrieval [68, 69]. The closest related work is [69], where the authors use the semantic neighborhood of multimodal models to identify samples with high semantic diversity using text-based neighbors of neighbors. However, as the objective of their work is different from ours, their proposed discrepancy and diversity scores would not provide a signal for label error in our setting. We further clarify this in Appendix B, and will empirically compare against their discrepancy score as a baseline. Although prior works have utilized the idea of multimodal neighbors in other settings, we believe we are the first to apply it to the setting of label error detection.

3 LEMON: Label Error Detection using Multimodal Neighbors

We are given a dataset $\mathcal{D} = \{(\mathbf{x}, \mathbf{y})_{i=1}^N\}$ consisting of two modalities $\mathbf{x} \in \mathcal{X}$ and $\mathbf{y} \in \mathcal{Y}$. For example, $\mathcal{X}$ may represent the set of all natural images, and $\mathcal{Y}$ may represent the set of all English text, or a restricted subset such as $\{\texttt{cat}, \texttt{dog}, ...\}$. We assume the existence of, but not access to, an oracle $f^* : \mathcal{X} \times \mathcal{Y} \to \{0, 1\}$, which is able to assign a binary mislabel indicator $z_i = f^*(\mathbf{x}_i, \mathbf{y}_i)$ to each sample in $\mathcal{D}$, without ambiguity. Here, $z_i = 1$ indicates that the sample is mislabeled, and $z_i = 0$ indicates that the sample is correctly labeled. Our goal is to output a score $s \in \mathbb{R}$ with some model $s := f(\mathbf{x}, \mathbf{y})$ such that

$$\text{AUROC} = \mathbb{E}_{\substack{(\mathbf{x},\mathbf{y})\sim\mathbb{P}(\cdot|z=1) \\ (\mathbf{x}',\mathbf{y}')\sim\mathbb{P}(\cdot|z=0)}} [\mathbf{1}_{f(\mathbf{x},\mathbf{y})\geq f(\mathbf{x}',\mathbf{y}')}]$$

is maximized. Here, inspired by prior work [2, 82], we propose a method for f based on nearest neighbors, summarized in Figure 2. Suppose we have a query sample $(\mathbf{x}, \mathbf{y})$[2]. Define $B(\mathbf{x}, r) := \{x' \in \mathcal{X} : d_{\mathcal{X}}(\mathbf{x}, \mathbf{x}') \leq r\}$, and $B(\mathbf{y}, r)$ similarly. Here, $r_k(x) := \inf\{r : |B(\mathbf{x}, r) \cap \mathcal{D}| \geq k\}$. Then, we define $\{\mathbf{x}_{n_1}, \mathbf{x}_{n_2}, ..., \mathbf{x}_{n_k}\} := B(\mathbf{x}, r_k(x)) \cap D$ the top k nearest neighbors of $\mathbf{x}$, and

[2]One could take, for any i, $(\mathbf{x}, \mathbf{y}) := (\mathbf{x}, \mathbf{y})_i$, $D' := D \setminus \{(\mathbf{x}, \mathbf{y})_i\}$

$\{\mathbf{y}_{m_1}, \mathbf{y}_{m_2}, ..., \mathbf{y}_{m_k}\} := B(\mathbf{y}, r_k(y)) \cap D$ the top k nearest neighbors of $\mathbf{y}$[3]. We assume that the neighbors are sorted in order of ascending distance, so for e.g. $d_{\mathcal{X}}(\mathbf{x}, \mathbf{x}_{n_2}) \geq d_{\mathcal{X}}(\mathbf{x}, \mathbf{x}_{n_1})$.

If $\mathcal{Y}$ is a small discrete set, we could choose $d(\mathbf{y}, \mathbf{y}') = \mathbf{1}_{\mathbf{y}=\mathbf{y}'}$. If $\mathcal{X}$ or $\mathcal{Y}$ are unstructured or high dimensional, we assume access to multimodal encoders $h_\theta = (h_\theta^{\mathcal{X}}, h_\theta^{\mathcal{Y}})$, where $h_\theta^{\mathcal{X}} : \mathcal{X} \to \mathbb{R}^d$ and $h_\theta^{\mathcal{Y}} : \mathcal{Y} \to \mathbb{R}^d$. Here, h_θ may be a CLIP model [59] trained on a large internet corpus, or, as we show later, it may be sufficient to train h_θ from scratch only on $\mathcal{D}$. Then, we could naturally use simple distance metrics in the embedding space, such as the cosine distance $d_{\mathcal{X}}(\mathbf{x}, \mathbf{x}') = d_{\cos}(h_\theta^{\mathcal{X}}(\mathbf{x}), h_\theta^{\mathcal{X}}(\mathbf{x}')) = 1 - \frac{h_\theta^{\mathcal{X}}(\mathbf{x}) \cdot h_\theta^{\mathcal{X}}(\mathbf{x}')}{||h_\theta^{\mathcal{X}}(\mathbf{x})||_2 \cdot ||h_\theta^{\mathcal{X}}(\mathbf{x}')||_2}$. Our proposed score is the linear combination of three terms:

$$s = f(\mathbf{x}, \mathbf{y}) = d_{mm}(\mathbf{x}, \mathbf{y}) + \beta s_n(\mathbf{x}, \mathbf{y}, \mathcal{D}) + \gamma s_m(\mathbf{x}, \mathbf{y}, \mathcal{D}) \tag{1}$$

Where $\beta, \gamma \geq 0$ are hyperparameters. Here, $d_{mm}(\mathbf{x}, \mathbf{y}) := d_{\cos}(h_\theta^{\mathcal{X}}(\mathbf{x}), h_\theta^{\mathcal{Y}}(\mathbf{y}))$ is the multimodal distance, which has been shown to provide a meaningful signal in prior label error detection work [37, 30]. We thus use this distance as the basis, and augment it with two additional terms based on nearest neighbors:

$$s_n(\mathbf{x}, \mathbf{y}, \mathcal{D}) = \frac{1}{k} \sum_{j=1}^{k} d_{\mathcal{Y}}(\mathbf{y}, \mathbf{y}_{n_j}) e^{-\tau_{1,n} d_{\mathcal{X}}(\mathbf{x}, \mathbf{x}_{n_j})} e^{-\tau_{2,n} d_{mm}(\mathbf{x}_{n_j}, \mathbf{y}_{n_j})} \tag{2}$$

Where $(\mathbf{x}_{n_j}, \mathbf{y}_{n_j}) \in \mathcal{D}$, and $\tau_{1,n}, \tau_{2,n} \geq 0$ are hyperparameters. This corresponds to finding the nearest neighbors of $\mathbf{x}$ in $\mathcal{X}$ space, then averaging the distance between their *corresponding* modality in $\mathcal{Y}$ and $\mathbf{y}$. We weight this average with two additional terms. The $\tau_{1,n}$ term corresponds to downweighting neighbors which are far from $\mathbf{x}$. Intuitively, this is useful when k is too large for $\mathbf{x}$ and not all neighbors are relevant and can be thought of as an adaptive k. The $\tau_{2,n}$ term corresponds to downweighting neighbors which are themselves likely to be mislabeled. If $(\mathbf{x}_{n_j}, \mathbf{y}_{n_j})$ is itself mislabeled, then $d_{\mathcal{Y}}(\mathbf{y}, \mathbf{y}_{n_j})$ would contribute an erroneous signal to whether $(\mathbf{x}, \mathbf{y})$ is mislabeled, and we thus want to downweight those instances.

The third term is analogous to s_n, but uses neighbors of $\mathbf{y}$:

$$s_m(\mathbf{x}, \mathbf{y}, \mathcal{D}) = \frac{1}{k} \sum_{j=1}^{k} d_{\mathcal{X}}(\mathbf{x}, \mathbf{x}_{m_j}) e^{-\tau_{1,m} d_{\mathcal{Y}}(\mathbf{y}, \mathbf{y}_{m_j})} e^{-\tau_{2,m} d_{mm}(\mathbf{x}_{m_j}, \mathbf{y}_{m_j})} \tag{3}$$

Where $(\mathbf{x}_{m_j}, \mathbf{y}_{m_j}) \in \mathcal{D}$, and $\tau_{1,m}, \tau_{2,m} \geq 0$ are hyperparameters. Crucially, note that $\mathbf{x}_{n_j} \neq \mathbf{x}_{m_j}$, and $\mathbf{y}_{n_j} \neq \mathbf{y}_{m_j}$. Specifically, $\mathbf{y}_{n_j}$ corresponds to the $\mathcal{Y}$ modality of nearest neighbors taken in $\mathcal{X}$ space, and $\mathbf{y}_{m_j}$ corresponds to the nearest neighbors of $\mathbf{y}$ taken in $\mathcal{Y}$ space.

We note that our method is a generalization of several prior methods. When $\beta = \gamma = 0$, the method is equivalent to CLIP similarity [37]. When β is large, $\tau_{1,n} = \tau_{2,n} = \gamma = 0$, and $d(\mathbf{y}, \mathbf{y}_{n_j}) = \mathbf{1}_{\mathbf{y}=\mathbf{y}_{n_j}}$, the method is equivalent to Deep kNN [2].

Our method contains several hyperparameters: $k, \beta, \gamma, \tau_{1,n}, \tau_{2,n}, \tau_{1.m}$, and $\tau_{2,m}$. When there is a validation set with known labels, we perform a grid search over k, and use numerical optimization methods to search for an optimal value of the remaining hyperparameters which maximize performance on this set, which we describe further in Section 5.2. We refer to our method in this setting as $\text{LEMON}_{\text{OPT}}$.

When there is no labeled validation set available, we will show that our method is fairly robust to these hyperparameter choices, and that choosing a set of reasonable fixed values for these hyperparameters yields nearly comparable results. We refer to our method in this setting as $\text{LEMON}_{\text{FIX}}$.

4 Theoretical Analysis

First, we demonstrate that the embedding models trained via the contrastive multimodal objective are natural noisy label detectors.

Theorem 4.1 (Contrastive multimodal embedding models can detect noisy labels)**.** *Suppose $\mathcal{Y} = \mathbb{R}$. For a training dataset $\mathcal{D}$, Suppose $\hat{h}_\theta^{\mathcal{X}}(x)$ and $\hat{h}_\theta^{\mathcal{Y}}(y)$ are the two embeddings that minimize the empirical CLIP objective on this dataset. Then, for an input x and its corresponding positive*

[3]We will use a subscript n_j to index nearest neighbors in $\mathcal{X}$, and subscript m_j for neighbors in $\mathcal{Y}$.

counterpart y, assume there exists a noisy label y' such that $y' = y + \eta$ where $\eta \sim \mathcal{N}(0, \sigma^2)$ and $|\eta| \geq \epsilon$. Then the following holds with probability at least $1 - \delta$, where δ is a function of ϵ.

$$d_{mm}(\hat{h}_\theta^{\mathcal{X}}(x), \hat{h}_\theta^{\mathcal{Y}}(y)) \leq d_{mm}(\hat{h}_\theta^{\mathcal{X}}(x), \hat{h}_\theta^{\mathcal{Y}}(y'))$$

Therefore, we can see that multimodal embeddings are inherently capable of detecting mislabeled pairs, ensuring the distance between the embeddings of positive pairs is smaller than that of negative pairs. This motivates the use of d_{mm} in LEMoN as well as in prior work [30, 37].

Next, we show that our multimodal kNN scores (Equations (**??**) and (**??**)) provide a signal for label error. Suppose there exists a "paraphrase function" $\mathcal{H} : \mathcal{Y} \to \mathcal{P}(\mathcal{Y})$, where $\mathcal{P}$ denotes the powerset, such that for a particular sample (x, y) with $\mathcal{H}(y) = (\bar{y}_1, \bar{y}_2...,)$, $(x, \bar{y}_i)$ is considered correctly labeled for all $\bar{y}_i \in \mathcal{H}(y)$. Informally, $\mathcal{H}$ outputs the set of all possible captions which correctly describe x. Similarly define $\mathcal{J}(x)$, which outputs the set of images with identical semantics as x.

Assumption 1 (Structure of $\mathcal{H}$, $\mathcal{J}$):

- Let (x', y') be an arbitrary sample. If $y' \notin \mathcal{H}(y)$, then $x' \notin \mathcal{J}(x)$.
- Let (x', y') be an arbitrary mislabeled sample. Then, $\forall y'' \in \mathcal{H}(y')$, $x'' \notin \mathcal{J}(x')$.

Assumption 2 (Distribution of Distances): *Let (X, Y) be a randomly drawn sample.*

- $\forall\ X' \notin \mathcal{J}(X) : d_{\mathcal{X}}(X, X') \overset{\text{iid}}{\sim} \mathcal{N}(\mu_1, \sigma_1^2)$.
- $\forall\ \bar{X} \in \mathcal{J}(X) : d_{\mathcal{X}}(X, \bar{X}) \overset{\text{iid}}{\sim} \mathcal{N}(\mu_2, \sigma_2^2)$.

We empirically validate this assumption in Appendix A.5.

Let $N_k(Y) = \{Y_{m_1}, ..., Y_{m_k}\}$ denote the nearest neighbors of Y in the text space. Let $\frac{1}{k}|\mathcal{H}(Y) \cap N_k(Y)| = \zeta_Y$, a random variable. Let $\mathbb{P}((X_{m_i}, Y_{m_i}) \text{ is mislabeled}) = p$.

Let $S_m(X, Y) = \frac{1}{k} \sum_{Y_{m_i} \in N_k(Y)} d_{\mathcal{X}}(X, X_{m_i})$, which is identical to the proposed Equation (**??**) with $\tau_1 = \tau_2 = 0$.

Theorem 4.2 (AUROC of kNN Score)**.** *Let (X, Y) be a randomly selected correctly labeled sample, and (X', Y') a randomly selected incorrectly labeled sample. Under Assumptions 1 and 2:*

$$\mathbb{P}(S_m(X', Y') > S_m(X, Y)) = 1 - \Phi(\frac{-\mu}{\sigma})$$

where $\mu = \mathbb{E}[\zeta_Y](1-p)(\mu_1 - \mu_2), \sigma = \sqrt{\frac{\mathbb{E}[\zeta_Y](1-p)\sigma_2^2 + (2 - \mathbb{E}[\zeta_Y](1-p))\sigma_1^2}{k} + \text{Var}(\zeta_Y)(1-p)^2(\mu_2 - \mu_1)^2}$, and Φ is the Gaussian CDF.

This provides an expression for the detection AUROC of the score S_m. The same expression can be derived for S_n by symmetry.

Lemma 4.3 (Non-random Signal of kNN Score)**.** *If the following three conditions hold: (1) $p < 1$, (2) $\mathbb{E}[\zeta_Y] > 0$, (3) $\mu_1 > \mu_2$. Then,*

$$\mathbb{P}(S_m(X', Y') > S_m(X, Y)) > 0.5$$

Under these conditions, S_m, our proposed multimodal neighborhood score, provides a better than random signal at detecting mislabeled samples. Full proofs can be found in Appendix A.

5 Experiments

5.1 Datasets

We evaluate our method using eight datasets, as shown in Table 1. Four datasets (`cifar10`, `cifar100`, `stanfordCars`, `miniImageNet`) are label error detection datasets from the classification setting. The four remaining datasets are image captioning datasets. For `mscoco` and `flickr30k`, we use the Karpathy split [31]. In the remaining datasets, we randomly split each dataset into three parts in an 80-10-10 ratio: training or reference set for the label detection method, validation set for hyperparameter selection, and test set for testing label error detection performance.

Table 1: Classification and captioning datasets. n is the number of samples. In the main paper, results shown are for the bolded noise type with 40% noise level for synthetic noise. Performance on remaining noise types can be found in the appendices.

Dataset	n			Domain		Noise Types
	Train	Validation	Test	Image	Text	
`cifar10`	40,000	5,000	5,000	Natural images	Object labels	{***human*** [75], *sym., asym.*}
`cifar100`	40,000	5,000	5,000	Natural images	Object labels	{***human*** [75], *sym., asym.*}
`miniImageNet` [28]	49,419	24,710	24,710	Natural images	Object labels	{***real***}
`stanfordCars` [28]	13,501	6,751	6,752	Car images	Car year and model	{***real***}
`mscoco` [42]	82,783	5,000	5,000	Natural images	Captions	{***cat.***, *noun*, *random*}
`flickr30k` [78]	29,000	1,014	1,000	Natural images	Captions	{***noun***, *random*}
`mmimdb` [1]	15,552	2,608	7,799	Movie Posters	Plot summaries	{***cat.***, *noun*, *random*}
`mimiccxr` [29]	368,909	2,991	5,159	Chest X-rays	Radiology reports	{***cat.***, *random*}

5.1.1 Noise Types

In `cifar10` and `cifar100`, we utilize a dataset collected in prior work [75] with human mislabels (*human*). We also follow prior work [82] in experimenting with class symmetric (*sym.*) and class asymmetric (*asym.*) synthetic noise. For `stanfordCars` and `miniimagenet`, we use datasets from [28], which contain noise from real-world (*real*) web annotators .

For the four captioning datasets, we devise several ways to inject synthetic noise of prevalence p. The simplest way is to randomly select p fraction (*random*) of the samples and assign their text modality to be that of another random caption. In datasets where additional metadata is available (`mscoco`: object category, `mmimdb`: genre of movie, `mimiccxr`: disease label), we can randomly swap the caption with that of another sample from the same category (*cat*). Finally, in all captioning datasets except `mimiccxr`, we tag each token of each caption with its part-of-speech using SpaCy [23], and then randomly assign a selected sample's text modality to be from another sample with at least one noun in common (*noun*). Dataset processing details are also in Appendix D.

Our motivation for these noise types is to simulate an array of realistic label corruptions that one might face in the real world. We recognize that the resulting synthetic dataset may not have exact noise level p, as e.g. a randomly selected caption may actually be correct for the image, as well as noise in the base datasets, which we explore in Section 6.4. Unless otherwise stated, results shown in the main paper are for the bolded noise type in Table 1, with 40% synthetic noise. Additional results for other noise types can be found in the appendices.

5.2 Model Selection and Evaluation

We run LEMoN on each dataset, using the training split of each dataset to compute nearest neighbors. In classification datasets, we use the discrete metric $d_{\mathcal{Y}}(\mathbf{y}, \mathbf{y}') = \mathbf{1}_{\mathbf{y}=\mathbf{y}'}$. In all other cases and for $d_{\mathcal{X}}$, we utilize cosine or euclidean distance computed in the embedding space of a pretrained CLIP model, selecting the best distance metric on the validation set for $\text{LEMoN}_{\text{OPT}}$, and keeping the distance as the cosine distance for $\text{LEMoN}_{\text{FIX}}$. In `mimiccxr`, we use BiomedCLIP (ViT-B/16) [81], and we use OpenAI CLIP ViT-B/32 [59] for all other datasets. A full list of hyperparameters for our method and the baselines are in Appendix G.

For $\text{LEMoN}_{\text{OPT}}$, we select the hyperparameter combination that maximizes F1 on a labeled validation set. We report the AUROC, AUPRC, and F1 for this model. For $\text{LEMoN}_{\text{FIX}}$, we fix the hyperparameters at the following reasonable values: $k = 30$, $\beta = \gamma = 5$, $\tau_{1,n} = \tau_{1,m} = 0.1$, and $\tau_{2,n} = \tau_{2,m} = 5$. We report AUROC and AUPRC, as the F1 requires additional information to compute a threshold for the score. We recognize that access to such a validation set as in $\text{LEMoN}_{\text{OPT}}$ may be unrealistic, but we will empirically show that (1) our method is fairly robust to selection of these hyperparameters, (2) only a few hundred labeled samples may be sufficient to select these hyperparameters, (3) using $\text{LEMoN}_{\text{FIX}}$ with the fixed hyperparameter setting described above achieves nearly comparable results, and (4) hyperparameters optimized on a dataset with synthetic noise may transfer well to real datasets.

We repeat each experiment three times, using a different random seed for the noise sampling (for *human* and *real* noise, we use a different random data split). Performance metrics shown are test-set results averaged over these three runs, with error bounds corresponding to one standard deviation.

Baselines We compare our method versus previous state-of-the-art in both the classification and captioning settings. We additionally adapt several baselines from the classification setting to the captioning setting. We briefly list the baselines here, and a detailed description is in the Appendix E.

Table 2: Label error detection performance across classification datasets. We separate AUM, Datamap, and Confident learning, as they require training a classifier from scratch. Bold denotes best score within each training approach. A full version of this table with AUPRC can be found in Appendix I.1.

Method	`cifar10`		`cifar100`		`miniImageNet`		`stanfordCars`	
	AUROC	**F1**	**AUROC**	**F1**	**AUROC**	**F1**	**AUROC**	**F1**
AUM	**98.3** (0.1)	**94.0** (0.1)	**92.2** (0.2)	**83.8** (0.4)	83.1 (0.2)	75.3 (0.2)	70.5 (2.4)	62.3 (1.2)
Datamap	98.2 (0.1)	93.4 (0.5)	91.8 (0.2)	83.5 (0.6)	**85.0** (0.2)	**77.0** (0.2)	**72.3** (1.8)	**64.9** (2.1)
Confident	93.7 (0.4)	92.7 (0.5)	74.1 (1.7)	69.3 (2.0)	70.5 (0.2)	54.7 (0.4)	61.0 (0.5)	43.4 (1.6)
CLIP Logits	95.5 (0.2)	88.0 (0.5)	84.9 (0.7)	75.5 (0.5)	90.0 (0.2)	**82.5** (0.2)	68.8 (0.7)	64.9 (0.4)
CLIP Sim.	93.8 (0.1)	86.9 (0.4)	78.5 (0.6)	69.2 (1.3)	89.3 (0.2)	81.3 (0.5)	69.8 (0.6)	61.7 (0.8)
Simifeat-V	90.6 (0.3)	88.0 (0.4)	79.5 (0.0)	73.1 (0.5)	68.2 (0.3)	55.0 (0.5)	63.7 (1.2)	43.7 (1.5)
Simifeat-R	90.7 (0.3)	88.1 (0.5)	79.7 (0.2)	73.6 (0.6)	68.0 (0.3)	54.7 (0.4)	63.5 (1.3)	43.4 (1.6)
Discrepancy	77.1 (1.9)	68.2 (1.9)	66.0 (1.5)	51.9 (1.8)	79.4 (0.3)	69.8 (0.4)	65.7 (0.7)	59.9 (0.4)
Deep k-NN	97.8 (0.1)	92.5 (0.5)	87.4 (0.3)	78.0 (0.3)	83.2 (0.2)	75.2 (0.4)	71.4 (0.6)	65.3 (0.9)
LEMON$_{\text{FIX}}$ (Ours)	97.7 (0.2)	-	88.9 (0.7)	-	89.5 (0.2)	-	72.6 (0.7)	-
LEMON$_{\text{OPT}}$ (Ours)	**98.1** (0.0)	**93.1** (0.2)	**90.8** (0.0)	**81.3** (0.2)	**90.2** (0.2)	**82.3** (0.1)	**73.1** (0.5)	**67.3** (1.0)

Classification In the classification setting, we experiment with the following baselines which require training a classifier on the particular dataset: **AUM** [57], **Datamap** [67], and **Confident Learning** [53], and the following baselines which do not require classifier training: **Deep k-NN** [2], **SimiFeat** [82]-Voting and Ranking, discrepancy in the image space (**Discrepancy**) (Υ_X^{DIS} from [69]) **CLIP Similarity** [30], and **CLIP Logits** [37, 14].

Captioning In the captioning setting, we compare our method with **LLaVA** [44] prompting (v1.6-vicuna-13b), and **CapFilt** [35]. We note that the latter can be viewed as an oracle for natural image captioning, as it has been trained in a supervised manner on clean `mscoco` data. **CLIP Similarity** [30], **Discrepancy** [69], and **Datamap** [67] can also be used directly in this setting. Finally, to adapt classification baselines to captioning, we embed the captions using the corresponding CLIP text encoder, and then use K-means clustering to assign the text caption into one of 100 clusters. We then apply **Deep k-NN** [2] and **Confident Learning** [53], using the cluster ID as the discretized class.

6 Results

Table 3: Label error detection performance on captioning datasets. Bold denotes best (highest) score. A full version of this table with AUPRC can be found in Appendix I.2.

Method	`flickr30k`		`mscoco`		`mmimdb`		`mimiccxr`	
	AUROC	**F1**	**AUROC**	**F1**	**AUROC**	**F1**	**AUROC**	**F1**
LLaVA	79.3 (0.8)	65.0 (1.1)	80.3 (0.1)	74.9 (0.3)	58.4 (0.2)	58.5 (0.1)	53.9 (0.5)	28.7 (0.1)
Datamap	54.0 (1.8)	28.2 (2.1)	49.9 (0.7)	28.6 (0.0)	50.1 (0.5)	28.9 (0.3)	50.2 (0.9)	28.9 (0.4)
Discrepancy	73.0 (0.6)	64.7 (1.7)	72.7 (0.3)	67.3 (0.9)	57.4 (0.4)	40.2 (1.7)	60.0 (0.8)	32.8 (2.8)
Deep k-NN	71.1 (0.4)	64.8 (2.7)	76.6 (0.4)	73.2 (0.3)	58.7 (0.7)	44.5 (1.0)	62.9 (0.4)	46.0 (4.4)
Confident	61.6 (0.5)	54.3 (0.8)	66.4 (1.2)	58.9 (1.5)	52.8 (0.8)	53.6 (0.7)	60.2 (0.3)	**59.4** (0.1)
CLIP Sim.	**94.8** (0.5)	**88.1** (0.7)	93.8 (0.2)	87.5 (0.3)	85.1 (0.3)	74.5 (0.3)	64.1 (0.4)	48.6 (3.4)
LEMON$_{\text{FIX}}$ (Ours)	93.6 (0.2)	-	92.0 (0.1)	-	84.3 (0.3)	-	66.5 (0.2)	-
LEMON$_{\text{OPT}}$ (Ours)	94.5 (0.2)	87.7 (0.9)	**95.6** (0.2)	**89.3** (0.2)	**86.0** (0.1)	**76.3** (0.1)	**70.4** (2.3)	57.0 (1.6)
CapFilt (Supervised Training)	98.6 (0.1)	94.8 (0.5)	99.3 (0.0)	96.2 (0.3)	82.7 (0.7)	71.6 (0.8)	49.2 (0.3)	28.5 (0.0)

6.1 LEMON Outperforms Baselines on Label Error Detection

Classification In Table 2, we show the performance of LEMON against the baselines for label error detection on classification datasets. We find that our method outperforms existing baselines which do not require classifier training on both CIFAR-10 and CIFAR-100. Two downstream-task specific approaches AUM and Datamap outperform all training-free models (particularly on CIFAR-10), but LEMON performs comparably (within 2%) to these methods, and is consistently within the top-3 methods. Similar results are also observed on the two synthetic error types (see Appendix Table I.2). We find that LEMON$_{\text{FIX}}$ performs almost comparably with LEMON$_{\text{OPT}}$.

Captioning In Table 3, we find that our method outperforms existing neighborhood and similarity-based baselines. Our model underperforms a fully supervised oracle-like model (CapFilt), where the supervision and training objective includes distinguishing between accurate and incorrect captions.

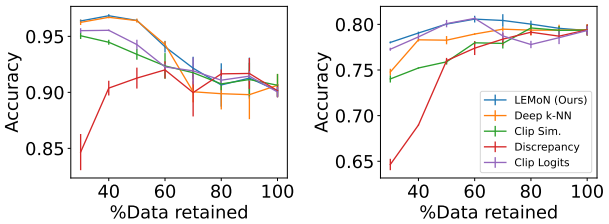

Figure 3: Downstream classification accuracy on `cifar10` (left) and `cifar100` (right) with LEMON$_{\text{OPT}}$ with *human* noise versus the baselines. Note that the noise prevalence is 40% in both datasets.

Dataset	Method	B@4	CIDER	ROUGE
flickr30k	No Filtering	28.1±1.1	64.6 ±2.6	49.6±0.7
	CLIP Sim.	29.7±1.0	71.8 ±1.8	50.7±0.5
	LEMON$_{\text{OPT}}$	29.6±0.9	71.2 ±2.0	50.7±0.6
	Clean	30.8±0.5	74.1 ±1.2	51.7±0.4
mscoco	No Filtering	35.1 ±0.4	116.7 ±1.5	56.4±0.4
	CLIP Sim.	37.9 ±0.4	126.7 ±0.7	58.4±0.3
	LEMON$_{\text{OPT}}$	38.4 ±0.2	127.3 ±0.2	58.5±0.1
	Clean	38.0 ±0.2	126.9±0.5	58.4±0.2

Table 4: Downstream captioning performance when removing 40% samples with highest mislabel scores. We observe that filtering noisy data with LEMON$_{\text{OPT}}$ improves captioning.

Results for synthetic error types show similar trends (see Appendix I.2). We present ablations of various components of LEMON in Table I.9,

Label Error Detection Performance Consistent Across Noise Ranges In Figure I.1, we show the performance of LEMON versus the CLIP similarity baseline on `mscoco` and `mmimdb`, varying the level of the synthetic noise. We find that our method performs better uniformly across noise levels.

Robustness to Hyperparameters Here, we test the robustness of our method when there is no labeled validation set available. First, in Appendix I.4, we visualize the F1 of the selected score when varying β and γ, keeping all other hyperparameters at their selected optimal values. We find that for most datasets and noise types, there is a reasonably large space of such hyperparameters, bounded away from the origin, which achieves close to optimal performance.

Next, we compare the performance of LEMON$_{\text{OPT}}$ and LEMON$_{\text{FIX}}$ with hyperparameters described in Section 5.2 across all datasets in Table I.8. We find that when there is no labeled validation set available, using these hyperparameters results in an AUROC drop of only 1.6% on average (std = 1.3%), with a worst-case AUROC drop of 3.9% across all 18 dataset and noise type combinations. Thus, even when a labeled validation set is not available, LEMON$_{\text{FIX}}$ with reasonable hyperparameter settings is able to outperform most baselines which do use such information.

6.2 Filtering Mislabeled Data Improves Downstream Performance

Classification To assess the impact of label error detection on the performance of the downstream classification tasks, we filter out samples from the training set with mislabel scores in the top q percentile. We vary q, train ViT [13] models on the filtered dataset, and evaluate the downstream test accuracy using clean data. In Figure 3, we find that training with LEMON$_{\text{OPT}}$ filtered samples leads to the highest accuracy on `cifar10` (96.84%), after removing more than 20% of the data. Training with LEMON$_{\text{OPT}}$ filtered samples is also on par with baselines on the other datasets (either outperforming or within 0.5% points of best baseline) as shown in Appendix I.12. Further, unlike other baselines, LEMoN is consistently in the top-2 best performing methods across all four datasets.

Captioning We finetune a pre-trained Huggingface checkpoint of a transformer decoder conditioned on CLIP image and text tokens – the GenerativeImage2Text (GIT) [73] model – to generate captions. Given the large size of the model, we use the parameter-efficient Low-Rank Adaptation (LoRA) [24] for all captioning models. We train models with clean data, noisy captions (*No Filtering*), and by filtering data detected as being mislabeled by a label detection method. In Table 4, we compare results of using either our model or a strong baseline (CLIP Sim.) for filtering data, as measured by the BLEU-4 [56], CIDER [72], and ROUGE [40] scores. In all cases, we filtered out the top-40% percentile of data predicted to be mislabeled (i.e., equal to the expected prevalence of noisy data). We find that (1) filtering out data predicted to be mislabeled helps recover performance as compared to training on fully clean data along multiple metrics, and (2) our method performs comparably to the baseline in improving downstream results, with some marginal improvements over CLIP Similarity on `mscoco`.

6.3 Is External Pretraining Required?

Thus far, all of the results for LEMON (and CLIP Similarity) have utilized CLIP models which have been pretrained on external datasets (e.g. PMC-15M in the case of BiomedCLIP). Here, we examine whether this is necessary, or whether we can achieve comparable performance by pretraining

Table 5: Performance of LEMoN versus the CLIP similarity baseline on `mimiccxr`, when external pretrained models may not be available. BiomedCLIP [80] is trained on a large corpus of biomedical image-text pairs. We find that pretraining only on noisy data from MIMIC-CXR outperforms BiomedCLIP, though pretraining on clean `mimiccxr` data (as in CheXzero [70]) does perform better.

		Random Noise			Cat. Noise		
		AUROC	**AUPRC**	**F1**	**AUROC**	**AUPRC**	**F1**
BiomedCLIP	Clip Sim.	66.8 (0.8)	54.4 (0.9)	54.3 (1.0)	64.1 (0.4)	51.7 (0.5)	48.6 (3.4)
	$\text{LEMoN}_{\text{FIX}}$ (Ours)	69.5 (0.7)	57.8 (1.0)	-	66.5 (0.2)	54.8 (0.4)	-
	$\text{LEMoN}_{\text{OPT}}$ (Ours)	73.1 (0.9)	63.0 (2.0)	63.1 (3.6)	70.4 (2.3)	60.3 (2.3)	57.0 (1.6)
CLIP Pretrain On Noisy Data	Clip Sim.	78.8 (0.1)	73.4 (0.5)	70.7 (0.5)	76.5 (0.5)	71.2 (0.4)	67.9 (0.7)
	$\text{LEMoN}_{\text{FIX}}$ (Ours)	80.5 (0.1)	76.1 (0.5)	-	77.0 (0.5)	72.4 (0.3)	-
	$\text{LEMoN}_{\text{OPT}}$ (Ours)	80.5 (0.1)	76.7 (0.3)	72.8 (0.7)	77.2 (0.8)	72.4 (0.6)	68.7 (0.2)
CheXzero	Clip Sim.	90.8 (0.0)	89.5 (0.0)	82.9 (0.2)	88.4 (0.6)	86.4 (0.7)	79.8 (0.7)
	$\text{LEMoN}_{\text{FIX}}$ (Ours)	91.4 (0.1)	90.4 (0.0)	-	88.4 (0.7)	87.0 (0.6)	-
	$\text{LEMoN}_{\text{OPT}}$ (Ours)	91.6 (0.3)	90.5 (0.4)	84.4 (0.5)	89.0 (0.3)	87.0 (0.6)	80.9 (0.6)

CLIP from scratch *only on the noisy data*. We select `mimiccxr` as it has the most samples out of all captioning datasets. Similar to CheXzero [70], we pretrain a CLIP ViT B/16 from scratch on the `mimiccxr` training set with 40% noise. We train this model for 10 epochs with a batch size of 64, and do not do any model selection or early stopping. We then apply LEMoN and the CLIP similarity baseline using this model, for the same noise level and noise type. We present our results in Table 5. Surprisingly, we find that pretraining CLIP only on noisy data from MIMIC-CXR actually outperforms BiomedCLIP. This could be attributed to the pretraining domain (chest X-rays and radiology notes) matching the inference domain exactly [52]. As an upper bound, we evaluate the same methods using CheXzero [70], which has been pretrained on *clean* MIMIC-CXR data. We find that, as expected, it far outperforms our method. We conclude that, for large noisy datasets, pretraining a CLIP model from scratch could be a viable solution, though pretraining on clean data from the same domain is certainly superior.

6.4 Real-World Analysis

We conduct a preliminary study of LEMoN on real datasets without known label errors. We run $\text{LEMoN}_{\text{FIX}}$ and the CLIP similarity baseline on `cifar10`, `cifar100`, `flickr30k`, and `mscoco`. As no labeled validation set is available, we use optimal hyperparameters from models previously run on each dataset with synthetic noise from Section 6.1 (shown in Appendix I.9). For each dataset, we select the top 200 images from the validation and test splits with the highest mislabel scores. We then manually annotated each sample to determine whether it was mislabeled. During labeling, images were randomly selected, so the labeler is unaware of whether the candidate image originated from the baseline or our method. We present the accuracy of each method in Table I.14. We find that our method outperforms the baseline for every dataset, though we recognize that this is a small-scale study and that many images are ambiguous. Examples of real-world mislabels can be found in Figures 1 and I.5. We present a further comparison of our identified error sets in `cifar10` and `cifar100` with a prior work [54] which obtained crowd-sourced labels for these datasets in Appendix I.11.

7 Conclusion

In this work, we proposed LEMoN, a novel method that leverages the neighborhood structure of contrastively pretrained multimodal embeddings to automatically identify label errors in image-text datasets. Through experiments on multiple datasets with synthetic and real-world noise, we demonstrated LEMoN's effectiveness in detecting label errors and its ability to improve downstream model performance when used as a dataset filtering tool.

Limitations In this work, we primarily rely on existing open-sourced datasets. While some parts of these datasets may have been used as training data in large pretrained vision-language models, we specifically chose pre-trained models that take care not to include the test sets of such datasets. Further, we run experiments on a real-world healthcare dataset (`mimiccxr`) to verify our results. Additionally, we have not assessed label error detection on synthetic instance-dependent [82] noise, which is an area of future work. Finally, in our evaluations, we assume that there exists an oracle binary indicator for whether a sample is mislabeled. As we saw in practice, real-world mislabels contain much more uncertainty and ambiguity, e.g. due to blurry images and differing interpretations of text [54, 16, 5, 4, 20, 19]. Evaluating the effectiveness of our score as a measure of this uncertainty, in the case of a non-binary target, is an area of future work.

References

[1] John Arevalo, Thamar Solorio, Manuel Montes-y Gómez, and Fabio A González. Gated multimodal units for information fusion. *arXiv preprint arXiv:1702.01992*, 2017.

[2] Dara Bahri, Heinrich Jiang, and Maya Gupta. Deep k-nn for noisy labels. In *International Conference on Machine Learning*, pages 540–550. PMLR, 2020.

[3] Randall Balestriero, Mark Ibrahim, Vlad Sobal, Ari Morcos, Shashank Shekhar, Tom Goldstein, Florian Bordes, Adrien Bardes, Gregoire Mialon, Yuandong Tian, et al. A cookbook of self-supervised learning. *arXiv preprint arXiv:2304.12210*, 2023.

[4] Valerio Basile, Federico Cabitza, Andrea Campagner, and Michael Fell. Toward a perspectivist turn in ground truthing for predictive computing. *arXiv preprint arXiv:2109.04270*, 2021.

[5] Lucas Beyer, Olivier J Hénaff, Alexander Kolesnikov, Xiaohua Zhai, and Aäron van den Oord. Are we done with imagenet? *arXiv preprint arXiv:2006.07159*, 2020.

[6] Shaotian Cai, Liping Qiu, Xiaojun Chen, Qin Zhang, and Longteng Chen. Semantic-enhanced image clustering. In *Proceedings of the AAAI conference on artificial intelligence*, volume 37, pages 6869–6878, 2023.

[7] Soravit Changpinyo, Piyush Sharma, Nan Ding, and Radu Soricut. Conceptual 12m: Pushing web-scale image-text pre-training to recognize long-tail visual concepts. In *Proceedings of the IEEE/CVF conference on computer vision and pattern recognition*, pages 3558–3568, 2021.

[8] Hao Chen, Jindong Wang, Ankit Shah, Ran Tao, Hongxin Wei, Xing Xie, Masashi Sugiyama, and Bhiksha Raj. Understanding and mitigating the label noise in pre-training on downstream tasks. *arXiv preprint arXiv:2309.17002*, 2023.

[9] Shan Chen, Jack Gallifant, Mingye Gao, Pedro Moreira, Nikolaj Munch, Ajay Muthukkumar, Arvind Rajan, Jaya Kolluri, Amelia Fiske, Janna Hastings, et al. Cross-care: Assessing the healthcare implications of pre-training data on language model bias. *arXiv preprint arXiv:2405.05506*, 2024.

[10] Ting Chen, Simon Kornblith, Mohammad Norouzi, and Geoffrey Hinton. A simple framework for contrastive learning of visual representations. In *International conference on machine learning*, pages 1597–1607. PMLR, 2020.

[11] Zijun Cui, Yong Zhang, and Qiang Ji. Label error correction and generation through label relationships. In *Proceedings of the AAAI Conference on Artificial Intelligence*, volume 34, pages 3693–3700, 2020.

[12] James Diffenderfer, Brian Bartoldson, Shreya Chaganti, Jize Zhang, and Bhavya Kailkhura. A winning hand: Compressing deep networks can improve out-of-distribution robustness. *Advances in neural information processing systems*, 34:664–676, 2021.

[13] Alexey Dosovitskiy, Lucas Beyer, Alexander Kolesnikov, Dirk Weissenborn, Xiaohua Zhai, Thomas Unterthiner, Mostafa Dehghani, Matthias Minderer, Georg Heigold, Sylvain Gelly, et al. An image is worth 16x16 words: Transformers for image recognition at scale. In *International Conference on Learning Representations*, 2020.

[14] Chen Feng, Georgios Tzimiropoulos, and Ioannis Patras. Clipcleaner: Cleaning noisy labels with clip. In *ACM Multimedia 2024*.

[15] Zhongtian Fu, Kefei Song, Luping Zhou, and Yang Yang. Noise-aware image captioning with progressively exploring mismatched words. In *Proceedings of the AAAI Conference on Artificial Intelligence*, volume 38, pages 12091–12099, 2024.

[16] Bin-Bin Gao, Chao Xing, Chen-Wei Xie, Jianxin Wu, and Xin Geng. Deep label distribution learning with label ambiguity. *IEEE Transactions on Image Processing*, 26(6):2825–2838, 2017.

[17] Roman Johannes Gertz, Thomas Dratsch, Alexander Christian Bunck, Simon Lennartz, Andra-Iza Iuga, Martin Gunnar Hellmich, Thorsten Persigehl, Lenhard Pennig, Carsten Herbert Gietzen, Philipp Fervers, et al. Potential of gpt-4 for detecting errors in radiology reports: Implications for reporting accuracy. *Radiology*, 311(1):e232714, 2024.

[18] Asghar Ghasemi and Saleh Zahediasl. Normality tests for statistical analysis: a guide for non-statisticians. *International journal of endocrinology and metabolism*, 10(2):486, 2012.

[19] Mitchell L Gordon, Michelle S Lam, Joon Sung Park, Kayur Patel, Jeff Hancock, Tatsunori Hashimoto, and Michael S Bernstein. Jury learning: Integrating dissenting voices into machine learning models. In *Proceedings of the 2022 CHI Conference on Human Factors in Computing Systems*, pages 1–19, 2022.

[20] Mitchell L Gordon, Kaitlyn Zhou, Kayur Patel, Tatsunori Hashimoto, and Michael S Bernstein. The disagreement deconvolution: Bringing machine learning performance metrics in line with reality. In *Proceedings of the 2021 CHI Conference on Human Factors in Computing Systems*, pages 1–14, 2021.

[21] Andreas Grivas, Beatrice Alex, Claire Grover, Richard Tobin, and William Whiteley. Not a cute stroke: analysis of rule-and neural network-based information extraction systems for brain radiology reports. In *Proceedings of the 11th international workshop on health text mining and information analysis*, pages 24–37, 2020.

[22] Dan Hendrycks and Thomas Dietterich. Benchmarking neural network robustness to common corruptions and perturbations. In *International Conference on Learning Representations*, 2018.

[23] Matthew Honnibal and Ines Montani. spaCy 2: Natural language understanding with Bloom embeddings, convolutional neural networks and incremental parsing. To appear, 2017.

[24] Edward J Hu, Phillip Wallis, Zeyuan Allen-Zhu, Yuanzhi Li, Shean Wang, Lu Wang, Weizhu Chen, et al. Lora: Low-rank adaptation of large language models. In *International Conference on Learning Representations*, 2021.

[25] Jia Cheng Hu, Roberto Cavicchioli, and Alessandro Capotondi. Exploiting multiple sequence lengths in fast end to end training for image captioning. In *2023 IEEE International Conference on Big Data (BigData)*, pages 2173–2182. IEEE, 2023.

[26] Bin Huang, Feng He, Qi Wang, Hong Chen, Guohao Li, Zhifan Feng, Xin Wang, and Wenwu Zhu. Neighbor does matter: Global positive-negative sampling for vision-language pre-training. In *ACM Multimedia 2024*, 2024.

[27] Runhui Huang, Yanxin Long, Jianhua Han, Hang Xu, Xiwen Liang, Chunjing Xu, and Xiaodan Liang. Nlip: Noise-robust language-image pre-training. In *Proceedings of the AAAI Conference on Artificial Intelligence*, volume 37, pages 926–934, 2023.

[28] Lu Jiang, Di Huang, Mason Liu, and Weilong Yang. Beyond synthetic noise: Deep learning on controlled noisy labels. In *International conference on machine learning*, pages 4804–4815. PMLR, 2020.

[29] Alistair EW Johnson, Tom J Pollard, Nathaniel R Greenbaum, Matthew P Lungren, Chih-ying Deng, Yifan Peng, Zhiyong Lu, Roger G Mark, Seth J Berkowitz, and Steven Horng. Mimic-cxr-jpg, a large publicly available database of labeled chest radiographs. *arXiv preprint arXiv:1901.07042*, 2019.

[30] Wooyoung Kang, Jonghwan Mun, Sungjun Lee, and Byungseok Roh. Noise-aware learning from web-crawled image-text data for image captioning. In *Proceedings of the IEEE/CVF International Conference on Computer Vision*, pages 2942–2952, 2023.

[31] Andrej Karpathy and Li Fei-Fei. Deep visual-semantic alignments for generating image descriptions. In *Proceedings of the IEEE conference on computer vision and pattern recognition*, pages 3128–3137, 2015.

[32] Taehyeon Kim, Jongwoo Ko, JinHwan Choi, Se-Young Yun, et al. Fine samples for learning with noisy labels. *Advances in Neural Information Processing Systems*, 34:24137–24149, 2021.

[33] Zhengfeng Lai, Noranart Vesdapunt, Ning Zhou, Jun Wu, Cong Phuoc Huynh, Xuelu Li, Kah Kuen Fu, and Chen-Nee Chuah. Padclip: Pseudo-labeling with adaptive debiasing in clip for unsupervised domain adaptation. In *Proceedings of the IEEE/CVF International Conference on Computer Vision*, pages 16155–16165, 2023.

[34] Junnan Li, Dongxu Li, Silvio Savarese, and Steven Hoi. Blip-2: Bootstrapping language-image pre-training with frozen image encoders and large language models. In *International conference on machine learning*, pages 19730–19742. PMLR, 2023.

[35] Junnan Li, Dongxu Li, Caiming Xiong, and Steven Hoi. Blip: Bootstrapping language-image pre-training for unified vision-language understanding and generation. In *International conference on machine learning*, pages 12888–12900. PMLR, 2022.

[36] Yangguang Li, Feng Liang, Lichen Zhao, Yufeng Cui, Wanli Ouyang, Jing Shao, Fengwei Yu, and Junjie Yan. Supervision exists everywhere: A data efficient contrastive language-image pre-training paradigm. In *International Conference on Learning Representations*, 2021.

[37] Chao Liang, Linchao Zhu, Humphrey Shi, and Yi Yang. Combating label noise with a general surrogate model for sample selection. *arXiv preprint arXiv:2310.10463*, 2023.

[38] Victor Weixin Liang, Yuhui Zhang, Yongchan Kwon, Serena Yeung, and James Y Zou. Mind the gap: Understanding the modality gap in multi-modal contrastive representation learning. *Advances in Neural Information Processing Systems*, 35:17612–17625, 2022.

[39] Thomas Liao, Rohan Taori, Inioluwa Deborah Raji, and Ludwig Schmidt. Are we learning yet? a meta review of evaluation failures across machine learning. In *Thirty-fifth Conference on Neural Information Processing Systems Datasets and Benchmarks Track (Round 2)*, 2021.

[40] Chin-Yew Lin. Rouge: A package for automatic evaluation of summaries. In *Text summarization branches out*, pages 74–81, 2004.

[41] Kevin Lin, Linjie Li, Chung-Ching Lin, Faisal Ahmed, Zhe Gan, Zicheng Liu, Yumao Lu, and Lijuan Wang. Swinbert: End-to-end transformers with sparse attention for video captioning. In *Proceedings of the IEEE/CVF Conference on Computer Vision and Pattern Recognition*, pages 17949–17958, 2022.

[42] Tsung-Yi Lin, Michael Maire, Serge Belongie, James Hays, Pietro Perona, Deva Ramanan, Piotr Dollár, and C Lawrence Zitnick. Microsoft coco: Common objects in context. In *Computer Vision–ECCV 2014: 13th European Conference, Zurich, Switzerland, September 6-12, 2014, Proceedings, Part V 13*, pages 740–755. Springer, 2014.

[43] Bingbin Liu, Sebastien Bubeck, Ronen Eldan, Janardhan Kulkarni, Yuanzhi Li, Anh Nguyen, Rachel Ward, and Yi Zhang. Tinygsm: achieving> 80% on gsm8k with small language models. *arXiv preprint arXiv:2312.09241*, 2023.

[44] Haotian Liu, Chunyuan Li, Qingyang Wu, and Yong Jae Lee. Visual instruction tuning. *Advances in neural information processing systems*, 36, 2024.

[45] Shayne Longpre, Gregory Yauney, Emily Reif, Katherine Lee, Adam Roberts, Barret Zoph, Denny Zhou, Jason Wei, Kevin Robinson, David Mimno, et al. A pretrainer's guide to training data: Measuring the effects of data age, domain coverage, quality, & toxicity. *arXiv preprint arXiv:2305.13169*, 2023.

[46] Ilya Loshchilov and Frank Hutter. Decoupled weight decay regularization. In *International Conference on Learning Representations*, 2018.

[47] Alexandra Sasha Luccioni and David Rolnick. Bugs in the data: How imagenet misrepresents biodiversity. In *Proceedings of the AAAI Conference on Artificial Intelligence*, volume 37, pages 14382–14390, 2023.

[48] Cristina Menghini, Andrew Delworth, and Stephen Bach. Enhancing clip with clip: Exploring pseudolabeling for limited-label prompt tuning. *Advances in Neural Information Processing Systems*, 36:60984–61007, 2023.

[49] Ishan Misra and Laurens van der Maaten. Self-supervised learning of pretext-invariant representations. In *Proceedings of the IEEE/CVF conference on computer vision and pattern recognition*, pages 6707–6717, 2020.

[50] Ryumei Nakada, Halil Ibrahim Gulluk, Zhun Deng, Wenlong Ji, James Zou, and Linjun Zhang. Understanding multimodal contrastive learning and incorporating unpaired data. In *International Conference on Artificial Intelligence and Statistics*, pages 4348–4380. PMLR, 2023.

[51] Nagarajan Natarajan, Inderjit S Dhillon, Pradeep K Ravikumar, and Ambuj Tewari. Learning with noisy labels. *Advances in neural information processing systems*, 26, 2013.

[52] Thao Nguyen, Gabriel Ilharco, Mitchell Wortsman, Sewoong Oh, and Ludwig Schmidt. Quality not quantity: On the interaction between dataset design and robustness of clip. *Advances in Neural Information Processing Systems*, 35:21455–21469, 2022.

[53] Curtis Northcutt, Lu Jiang, and Isaac Chuang. Confident learning: Estimating uncertainty in dataset labels. *Journal of Artificial Intelligence Research*, 70:1373–1411, 2021.

[54] Curtis G Northcutt, Anish Athalye, and Jonas Mueller. Pervasive label errors in test sets destabilize machine learning benchmarks. *arXiv preprint arXiv:2103.14749*, 2021.

[55] Aaron van den Oord, Yazhe Li, and Oriol Vinyals. Representation learning with contrastive predictive coding. *arXiv preprint arXiv:1807.03748*, 2018.

[56] Kishore Papineni, Salim Roukos, Todd Ward, and Wei-Jing Zhu. Bleu: a method for automatic evaluation of machine translation. In *Proceedings of the 40th annual meeting of the Association for Computational Linguistics*, pages 311–318, 2002.

[57] Geoff Pleiss, Tianyi Zhang, Ethan Elenberg, and Kilian Q Weinberger. Identifying mislabeled data using the area under the margin ranking. *Advances in Neural Information Processing Systems*, 33:17044–17056, 2020.

[58] Bryan A Plummer, Liwei Wang, Chris M Cervantes, Juan C Caicedo, Julia Hockenmaier, and Svetlana Lazebnik. Flickr30k entities: Collecting region-to-phrase correspondences for richer image-to-sentence models. In *Proceedings of the IEEE international conference on computer vision*, pages 2641–2649, 2015.

[59] Alec Radford, Jong Wook Kim, Chris Hallacy, Aditya Ramesh, Gabriel Goh, Sandhini Agarwal, Girish Sastry, Amanda Askell, Pamela Mishkin, Jack Clark, et al. Learning transferable visual models from natural language supervision. In *International conference on machine learning*, pages 8748–8763. PMLR, 2021.

[60] Tal Ridnik, Emanuel Ben-Baruch, Asaf Noy, and Lihi Zelnik-Manor. Imagenet-21k pretraining for the masses. *Proceedings of 35th Conference on Neural Information Processing Systems, Track on Datasets and Benchmarks*, 2021.

[61] Olga Russakovsky, Jia Deng, Hao Su, Jonathan Krause, Sanjeev Satheesh, Sean Ma, Zhiheng Huang, Andrej Karpathy, Aditya Khosla, Michael Bernstein, et al. Imagenet large scale visual recognition challenge. *International journal of computer vision*, 115:211–252, 2015.

[62] Simon Schrodi, David T Hoffmann, Max Argus, Volker Fischer, and Thomas Brox. Two effects, one trigger: On the modality gap, object bias, and information imbalance in contrastive vision-language representation learning. *arXiv preprint arXiv:2404.07983*, 2024.

[63] Florian Schroff, Dmitry Kalenichenko, and James Philbin. Facenet: A unified embedding for face recognition and clustering. In *Proceedings of the IEEE conference on computer vision and pattern recognition*, pages 815–823, 2015.

[64] Christoph Schuhmann, Richard Vencu, Romain Beaumont, Robert Kaczmarczyk, Clayton Mullis, Aarush Katta, Theo Coombes, Jenia Jitsev, and Aran Komatsuzaki. Laion-400m: Open dataset of clip-filtered 400 million image-text pairs. *arXiv preprint arXiv:2111.02114*, 2021.

[65] Peiyang Shi, Michael C Welle, Mårten Björkman, and Danica Kragic. Towards understanding the modality gap in clip. In *ICLR 2023 Workshop on Multimodal Representation Learning: Perks and Pitfalls*, 2023.

[66] Kihyuk Sohn. Improved deep metric learning with multi-class n-pair loss objective. *Advances in neural information processing systems*, 29, 2016.

[67] Swabha Swayamdipta, Roy Schwartz, Nicholas Lourie, Yizhong Wang, Hannaneh Hajishirzi, Noah A Smith, and Yejin Choi. Dataset cartography: Mapping and diagnosing datasets with training dynamics. *arXiv preprint arXiv:2009.10795*, 2020.

[68] Christopher Thomas and Adriana Kovashka. Preserving semantic neighborhoods for robust cross-modal retrieval. In *Computer Vision–ECCV 2020: 16th European Conference, Glasgow, UK, August 23–28, 2020, Proceedings, Part XVIII 16*, pages 317–335. Springer, 2020.

[69] Christopher Thomas and Adriana Kovashka. Emphasizing complementary samples for non-literal cross-modal retrieval. In *Proceedings of the IEEE/CVF Conference on Computer Vision and Pattern Recognition*, pages 4632–4641, 2022.

[70] Ekin Tiu, Ellie Talius, Pujan Patel, Curtis P Langlotz, Andrew Y Ng, and Pranav Rajpurkar. Expert-level detection of pathologies from unannotated chest x-ray images via self-supervised learning. *Nature Biomedical Engineering*, 6(12):1399–1406, 2022.

[71] Vijay Vasudevan, Benjamin Caine, Raphael Gontijo Lopes, Sara Fridovich-Keil, and Rebecca Roelofs. When does dough become a bagel? analyzing the remaining mistakes on imagenet. *Advances in Neural Information Processing Systems*, 35:6720–6734, 2022.

[72] Ramakrishna Vedantam, C Lawrence Zitnick, and Devi Parikh. Cider: Consensus-based image description evaluation. In *Proceedings of the IEEE conference on computer vision and pattern recognition*, pages 4566–4575, 2015.

[73] Jianfeng Wang, Zhengyuan Yang, Xiaowei Hu, Linjie Li, Kevin Lin, Zhe Gan, Zicheng Liu, Ce Liu, and Lijuan Wang. Git: A generative image-to-text transformer for vision and language. *Transactions on Machine Learning Research*, 2022.

[74] Yiyu Wang, Jungang Xu, and Yingfei Sun. End-to-end transformer based model for image captioning. In *Proceedings of the AAAI Conference on Artificial Intelligence*, volume 36, pages 2585–2594, 2022.

[75] Jiaheng Wei, Zhaowei Zhu, Hao Cheng, Tongliang Liu, Gang Niu, and Yang Liu. Learning with noisy labels revisited: A study using real-world human annotations. *arXiv preprint arXiv:2110.12088*, 2021.

[76] Pengxiang Wu, Songzhu Zheng, Mayank Goswami, Dimitris Metaxas, and Chao Chen. A topological filter for learning with label noise. *Advances in neural information processing systems*, 33:21382–21393, 2020.

[77] Kelvin Xu, Jimmy Ba, Ryan Kiros, Kyunghyun Cho, Aaron Courville, Ruslan Salakhudinov, Rich Zemel, and Yoshua Bengio. Show, attend and tell: Neural image caption generation with visual attention. In *International conference on machine learning*, pages 2048–2057. PMLR, 2015.

[78] Peter Young, Alice Lai, Micah Hodosh, and Julia Hockenmaier. From image descriptions to visual denotations: New similarity metrics for semantic inference over event descriptions. *Transactions of the Association for Computational Linguistics*, 2:67–78, 2014.

[79] Xiaohua Zhai, Joan Puigcerver, Alexander Kolesnikov, Pierre Ruyssen, Carlos Riquelme, Mario Lucic, Josip Djolonga, Andre Susano Pinto, Maxim Neumann, Alexey Dosovitskiy, et al. The visual task adaptation benchmark. 2019.

[80] Sheng Zhang, Yanbo Xu, Naoto Usuyama, Jaspreet Bagga, Robert Tinn, Sam Preston, Rajesh Rao, Mu Wei, Naveen Valluri, Cliff Wong, et al. Large-scale domain-specific pretraining for biomedical vision-language processing. *arXiv preprint arXiv:2303.00915*, 2(3):6, 2023.

[81] Sheng Zhang, Yanbo Xu, Naoto Usuyama, Hanwen Xu, Jaspreet Bagga, Robert Tinn, Sam Preston, Rajesh Rao, Mu Wei, Naveen Valluri, et al. Biomedclip: a multimodal biomedical foundation model pretrained from fifteen million scientific image-text pairs. *arXiv preprint arXiv:2303.00915*, 2023.

[82] Zhaowei Zhu, Zihao Dong, and Yang Liu. Detecting corrupted labels without training a model to predict. In *International conference on machine learning*, pages 27412–27427. PMLR, 2022.

A Theoretical results

A.1 CLIP as Noise Detector

In this section, we present a theoretical analysis of the impact of noisy labels in multimodal learning. Specifically, we illustrate that multimodal embeddings are robust when there is noise in one modality, which consequently can be leveraged as noisy detectors in our proposed method.

Let $\mathcal{X}$ and $\mathcal{Y}$ denote the input space of two modalities.

The objective of multimodal representation learning is to find an encoder for each modality: $h_\theta^{\mathcal{X}} : \mathcal{X} \to \mathbb{R}^d$, and $h_\theta^{\mathcal{Y}} : \mathcal{Y} \to \mathbb{R}^d$ simultaneously, which is usually realized by minimizing over multimodal contrastive learning loss such as CLIP loss [59]. We define the *multimodal distance* as $d_{mm}(h_\theta^{\mathcal{X}}(x), h_\theta^{\mathcal{Y}}(y))$ which measures the distance the embeddings from two modalities respectively. To further proceed with our analysis, we first define $y \in Y$ to be the correct label for x and $y' \in \mathcal{Y}$ be the noisy label obtained by flipping y with probability p, chosen uniformly at random from the set of incorrect labels $\mathcal{Y} \setminus \{y\}$. Additionally, we assume $h_\theta^{\mathcal{X}} : \mathcal{X} \mapsto \mathbb{R}^d$ and $h_\theta^{\mathcal{Y}} : \mathcal{Y} \mapsto \mathbb{R}^d$ to be Lipschitz continuous with Lipschitz constants $L_{\mathcal{X}}$ and $L_{\mathcal{Y}}$.

Proposition A.1. *Let the objective function $\mathcal{L}(h_\theta^{\mathcal{X}}, h_\theta^{\mathcal{Y}})$ be the CLIP loss:*

$$L(h_\theta^{\mathcal{X}}, h_\theta^{\mathcal{Y}}, \delta) = -\frac{1}{2}\left[\frac{1}{N}\sum_{i=1}^{N} \ln \frac{\exp(h_\theta^{\mathcal{X}}(x_i)^\top h_\theta^{\mathcal{Y}}(y_i)/\delta)}{\sum_{k=1}^{N}\exp(h_\theta^{\mathcal{X}}(x_k)^\top h_\theta^{\mathcal{Y}}(y_i)/\delta)} + \frac{1}{N}\sum_{i=1}^{N} \ln \frac{\exp(h_\theta^{\mathcal{X}}(x_i)^\top h_\theta^{\mathcal{Y}}(y_i)/\delta)}{\sum_{k=1}^{N}\exp(h_\theta^{\mathcal{X}}(x_i)^\top h_\theta^{\mathcal{Y}}(y_k)/\delta)}\right]$$

*Then the multimodal representation loss is **robust** to label noise and satisfies the following property:*

$$|L(h_\theta^{\mathcal{X}}(x), h_\theta^{\mathcal{Y}}(y)) - L(h_\theta^{\mathcal{X}}(x), h_\theta^{\mathcal{Y}}(y'))| \leq C\|h_\theta^{\mathcal{Y}}(y) - h_\theta^{\mathcal{Y}}(y')\|_2$$

where C is a constant.

The above proposition indicates that the CLIP loss change is bounded by the embedding *difference*, since it inherently provides robustness to noisy labels due to the properties of cosine similarity and Lipschitz continuity of the embedding functions. Such robustness enables a multimodal contrastive learning method to train meaningful embeddings under the presence of noisy input [65, 50]. We will empirically validate this in Section 6.3, by pretraining CLIP from scratch on noisy input.

Moreover, we demonstrate that the embedding models trained via the contrastive multimodal objective are natural noisy label detectors.

Theorem A.2 (Contrastive multimodal embedding models detect noisy labels)**.** *Suppose $\mathcal{Y} = \mathbb{R}$. For a training dataset $\mathcal{D}$, Suppose $\hat{h}_\theta^{\mathcal{X}}(x)$ and $\hat{h}_\theta^{\mathcal{Y}}(y)$ are the two embeddings that minimize the empirical CLIP objective on this dataset. Then, for an input x and its corresponding positive counterpart y, assume there exists a noisy label y' such that $y' = y + \eta$ where $\eta \sim \mathcal{N}(0, \sigma^2)$ and $|\eta| \geq \epsilon$. Then the following holds with probability at least $1 - \delta$, where δ is a function of ϵ.*

$$d_{mm}(\hat{h}_\theta^{\mathcal{X}}(x), \hat{h}_\theta^{\mathcal{Y}}(y)) \leq d_{mm}(\hat{h}_\theta^{\mathcal{X}}(x), \hat{h}_\theta^{\mathcal{Y}}(y'))$$

Therefore, we can see that multimodal embeddings are inherently capable of detecting mislabeled pairs, ensuring the distance between the embeddings of positive pairs is smaller than that of negative pairs. This motivates the use of d_{mm} in LEMoN as well as in prior work [30, 37].

A.2 Proof: Proposition A.1

Assumptions:

1. **Noise Model:** Let $y \in \mathcal{Y}$ be the correct text label and $y' \in Y$ be the noisy label obtained by flipping y with probability p, chosen uniformly at random from the set of incorrect labels $\mathcal{Y} \setminus \{y\}$. The noisy text embedding is denoted as $g'(y)$.
2. **Embedding Functions:** Assume $f : \mathcal{X} \to \mathbb{R}^d$ and $g : \mathcal{Y} \to \mathbb{R}^d$ are Lipschitz continuous functions with Lipschitz constants L_f and L_g, respectively. This means:
$$\|f(x_1) - f(x_2)\| \leq L_f(\|x_1 - x_2\|), \quad \forall x_1, x_2 \in \mathcal{X}$$
$$\|g(y_1) - g(y_2)\| \leq L_g(\|y_1 - y_2\|), \quad \forall y_1, y_2 \in \mathcal{Y}$$
3. **Robust Loss Function:** Let L be a robust loss function that satisfies the following property:
$$|L(f(x), g(y)) - L(f(x), g'(y))| \leq C(\|g(y) - g'(y)\|)$$
where C is a constant that depends on the specific choice of L.

Theorem: Under the above assumptions, the multimodal distance $D(f(x), g(y)) = \|f(x) - g(y)\|$ is robust to noise in the text modality, satisfying:

$$|D(f(x), g'(y)) - D(f(x), g(y))| \leq L_g C' p$$

where C' is a constant that depends on the properties of the embedding space and the set of incorrect labels.

Proof:

1. By the triangle inequality:

$$|D(f(x), g'(y)) - D(f(x), g(y))| \leq \|g'(y) - g(y)\|$$

2. Since g is Lipschitz continuous and y' is chosen uniformly at random from the set of incorrect labels $\mathcal{Y} \setminus \{y\}$:

$$\begin{aligned}\mathbb{E}[\|g(y') - g(y)\|] &\leq L_g \mathbb{E}[\|y' - y\|] \\ &\leq L_g \frac{1}{|Y| - 1} \sum_{y' \in Y \setminus \{y\}} \|y' - y\| \\ &\leq L_g C'\end{aligned}$$

   where C' depends on the properties of the embedding space and the set of incorrect labels.

3. By the linearity of expectation and the noise model

$$\begin{aligned}\mathbb{E}[\|g'(y) - g(y)\|] &= p\mathbb{E}[\|g(y') - g(y)\| \, |y' \neq y] + (1 - p)\mathbb{E}[\|g(y) - g(y)\| \, |y' = y] \\ &\leq p\mathbb{E}[\|g(y') - g(y)\|] \\ &\leq L_g C' p\end{aligned}$$

4. Combining steps 1 and 3:

$$\begin{aligned}|D(f(x), g'(y)) - D(f(x), g(y))| &\leq \|g'(y) - g(y)\| \\ &\leq \mathbb{E}[\|g'(y) - g(y)\|] \\ &\leq L_g C' p\end{aligned}$$

Therefore, the multimodal distance is robust to noise in the text modality, with the deviation bounded by $L_g C' p$.

A.3 Proof: Theorem 4.1

Consider the case where there is a batch of two pairs of samples. $\{(x, y), (x, y')\}$, where (x, y) are labelled as positive pairs and (x, y') are negative pairs, with $\|y - y'\| \geq \epsilon$. The empirical CLIP loss for this objective is

$$\mathcal{L}_{CLIP} = -2 \log \frac{\exp(h_x h_y^\top)}{\exp(h_x h_y^\top) + \exp(h_x {h'}_y^\top)}$$

Since we assume an optimal embedding that satisfies the CLIP objective to be $\hat{h}^X(x_i) := x_i$, $\hat{h}^Y(y_j) := x_i$ if $i = j$. Also this embedding model gives all embeddings with norm 1, $\|\hat{h}^x_\theta(x)\| = \|\hat{h}^y_\theta(y)\| = 1$. It can be shown that the above encoders minimize the above CLIP objective. Recall that the noisy label is considered as a negative pair (x, y') where $y' = y + \eta$ and $\eta \sim \mathcal{N}(0, \sigma^2 I)$ with $\|\eta\| \geq \epsilon$.

Given the above encoders, the cosine similarity for positive pairs is given as

$$\cos(\hat{h}^x_\theta(x), \hat{h}^y_\theta(y)) = \hat{h}^x_\theta(x) \cdot \hat{h}^y_\theta(y) = 1$$

And for the noise label

$$\cos(\hat{h}^x_\theta(x), \hat{h}^y_\theta(y')) = \hat{h}^x_\theta(x) \cdot \hat{h}^y_\theta(y') = \hat{h}^x_\theta(x) \cdot (y + \eta)$$

Since $y' = y + \eta$, we can find expectation $\mathbb{E}[\hat{h}^x_\theta(x) \cdot \eta] = 0$ and variance $\text{Var}(\hat{h}^x_\theta(x) \cdot \eta) = \sigma^2 \|\hat{h}^x_\theta(x)\|^2 = \sigma^2$, therefore $\mathbb{E}[\hat{h}^x_\theta(x) \cdot \hat{h}^y_\theta(y')] = \hat{h}^x_\theta(x) \cdot y = 1$.

Bounding the Cosine Similarity: The cosine similarity for negative pairs becomes:

$$\cos(\hat{h}_\theta^x(x), \hat{h}_\theta^y(y')) = \hat{h}_\theta^x(x) \cdot (y + \eta) = 1 + \hat{h}_\theta^x(x) \cdot \eta$$

For the similarity to be less than 1:

$$\hat{h}_\theta^x(x) \cdot \eta < 0$$

We want:

$$\mathbb{P}\left[\hat{h}_\theta^x(x) \cdot \eta < 0\right] = 1 - \mathbb{P}\left[\hat{h}_\theta^x(x) \cdot \eta \geq 0\right]$$

Using Chebyshev's Inequality: For $\hat{h}_\theta^x(x) \cdot \eta$:

$$\mathbb{P}\left[\hat{h}_\theta^x(x) \cdot \eta \geq \epsilon\right] \leq \frac{\sigma^2}{\epsilon^2}$$

Hence,

$$\mathbb{P}\left[(\hat{h}_\theta^x(x) \cdot \eta < \epsilon)\right] \geq 1 - \frac{\sigma^2}{\epsilon^2}$$

Using Chebyshev's inequality, we have:

$$\mathbb{P}\left[\cos(\hat{h}_\theta^x(x), \hat{h}_\theta^y(y)) > \cos(\hat{h}_\theta^x(x), \hat{h}_\theta^y(y'))\right] \geq 1 - \frac{\sigma^2}{\epsilon^2}$$

Therefore, we can show that given a pair of multimodal samples (x, y) and another one with noisy label (x, y'), the cosine similarity of the noisy labels will be smaller with a high probability. It is worth noticing that the existence of optimal multimodal encoders is a relatively strong assumption. Our theoretical analysis provides a clear implication for our proposed method and, in return, is empirically verified by our experimental results.

A.4 Proof: Theorem 4.2

For a correctly labeled sample (X, Y), We have that $k\zeta_Y(1-p)$ of the neighbors are relevant and have correct labels, and so each contribute $d_\mathcal{X}(X, \bar{X})$ to $S_m(X, Y)$, and all remaining samples are either incorrectly labeled, or are not relevant to Y, and so each contribute $d_\mathcal{X}(X, X')$. Since $S_m(X, Y)$ is the sum of iid Gaussians, it is also a Gaussian, with:

$$\begin{aligned}
\mathbb{E}[S_m(X,Y)] &= \frac{1}{k}\left(\mathbb{E}[\mathbb{E}[d(X,\bar{X}_1) + ... + d(X,\bar{X}_{k\zeta_Y(1-p)})|\zeta]] + \mathbb{E}[\mathbb{E}[d(X,X'_1) + ... + d(X,X'_{k-k\zeta_Y(1-p)})|\zeta]]\right) \\
&= \mathbb{E}[\zeta_Y](1-p)\mu_2 + (1 - \mathbb{E}[\zeta_Y](1-p))\mu_1 \\
&= \mathbb{E}[\zeta_Y](1-p)(\mu_2 - \mu_1) + \mu_1
\end{aligned}$$

$$\begin{aligned}
\mathrm{Var}[S_m(X,Y)] &= \mathbb{E}[\mathrm{Var}(S_m(X,Y)|\zeta_Y)] + \mathrm{Var}(\mathbb{E}[S_m(X,Y)|\zeta_Y]) \\
&= \mathbb{E}[\frac{1}{k}\left(\zeta_Y(1-p)\sigma_2^2 + (1 - \zeta_Y(1-p))\sigma_1^2\right)] + \mathrm{Var}(\zeta_Y(1-p)(\mu_2 - \mu_1) + \mu_1) \\
&= \frac{1}{k}\left(\mathbb{E}[\zeta_Y](1-p)\sigma_2^2 + (1 - \mathbb{E}[\zeta_Y](1-p))\sigma_1^2\right) + \mathrm{Var}(\zeta_Y)(1-p)^2(\mu_2 - \mu_1)^2
\end{aligned}$$

Similarly,

$$S(X', Y') \sim \mathcal{N}(\mu_1, \frac{\sigma_1^2}{k})$$

Putting it all together:

$$\mathbb{P}(S_m(X', Y') - S_m(X, Y) > 0) = 1 - \Phi(\frac{-\mu}{\sigma})$$

Where $\mu = \mathbb{E}[\zeta_Y](1-p)(\mu_1 - \mu_2)$, $\sigma = \sqrt{\frac{1}{k}\left(\mathbb{E}[\zeta_Y](1-p)\sigma_2^2 + (2 - \mathbb{E}[\zeta_Y](1-p))\sigma_1^2\right) + \mathrm{Var}(\zeta_Y)(1-p)^2(\mu_2 - \mu_1)^2}$, and Φ is the Gaussian CDF. Note that $\mathrm{Var}(\zeta_Y)$ is finite as ζ_Y is bounded by $[0, 1]$.
Setting $\mu > 0$ gives Lemma 4.3.

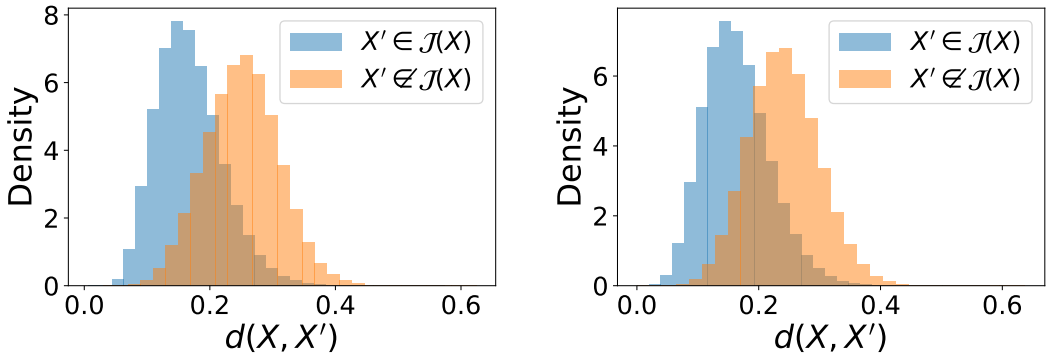

(a) CIFAR-10 (b) CIFAR-100

Figure A.1: Histogram of cosine distances in the CLIP image embedding space

A.5 Empirically Validating Assumption 2

To empirically validate Assumption 2, we utilize the training sets from the original CIFAR-10 and CIFAR-100 datasets. As these are classification datasets, we naturally define $\mathcal{J}$ as: $x_2 \in \mathcal{J}(x_1) \iff y_1 = y_2$, i.e. all images with the same label are paraphrases. We encode these images using the image encoder from OpenAI CLIP ViT-B/32 [59], and utilize the cosine distance as $d_{\mathcal{X}}$. We compute pairwise distance between all 40,000 samples, and categorize these distances into either $x' \in J(x)$ or $x' \notin J(x)$. We plot a histogram of these distances in Figure A.1. Visually, both of these distributions appear to be normal, and we also observe that $\mu_1 > \mu_2$ from Lemma 4.3. We then run a Shapiro–Wilk test on all four distributions to test for normality, randomly subsampling to 100 samples, as the Shapiro-Wilk test is not suitable for large sample sizes [18]. We find that in all four cases, the null hypothesis cannot be rejected ($p > 0.05$), and the test statistics are all greater than 0.97, indicating a high degree of normality.

B Comparison with [69]

The goal of [69] to identify samples with semantic diversity, which is different from our goal of identifying mislabeled examples. As such, their proposed scores (i.e. Υ^{DIS} and Υ^{DIV}) may not be effective in identifying mislabeled samples. As an example, consider the score Υ^{DIS}_{Y}, which computes the similarity between the original caption, and the captions of its second-degree neighbors in text-space. Given a particular caption, e.g. "This is a plane from the front view" in Figure 2, it could have second-degree neighbors in text-space that are semantically very similar to this caption (e.g. "A plane facing the viewer"). However, only computing the distance of these captions in text space does not provide any signal for whether the *image* is correctly paired to the caption. Similarly, the Υ^{DIV} scores also would not necessarily work, as the closeness of neighbors to each other in either modality do not provide a signal for whether the original sample is mislabeled.

However, the score from [69] that would intuitively provide a signal for mislabeling is Υ^{DIS}_{X}, which computes second-degree neighbors in text space, then examines similarity between images. This is essentially the sum over $d_{\mathcal{X}}(\mathbf{x}, \mathbf{x}_{m_j})$ terms in our Equation (**??**), but using second-degree neighbors instead of nearest neighbors. In addition, our Equation (**??**) contains two additional weighting terms (which we show improve label error performance in our ablation experiments). Finally, our proposed score contains the sum of two additional terms, which are not explored in [69].

We compare the performance of our method against the Υ^{DIS}_{X} score in the main paper, and show performance of all four scores from [69] in Appendix I.7.

C LEMoN Algorithm

[H] Dataset $\mathcal{D} = \{(\mathbf{x}_i, \mathbf{y}_i)\}_{i=1}^{N}$, Multimodal encoders $h_\theta^{\mathcal{X}}$, $h_\theta^{\mathcal{Y}}$, Distance functions $d_{\mathcal{X}}$, $d_{\mathcal{Y}}$
Hyperparameters: k, β, γ, $\tau_{1,n}$, $\tau_{2,n}$, $\tau_{1,m}$, $\tau_{2,m}$ Scores $\{s_i\}_{i=1}^{N}$

Cache embeddings $h_\theta^{\mathcal{X}}(\mathbf{x}_i)$ and $h_\theta^{\mathcal{Y}}(\mathbf{y}_i)$ for $(\mathbf{x}_i, \mathbf{y}_i) \in \mathcal{D}$ Cache $d_{mm}(\mathbf{x}_i, \mathbf{y}_i) = 1 - \frac{h_\theta^{\mathcal{X}}(\mathbf{x}_i) \cdot h_\theta^{\mathcal{Y}}(\mathbf{y}_i)}{\|h_\theta^{\mathcal{X}}(\mathbf{x}_i)\|_2 \|h_\theta^{\mathcal{Y}}(\mathbf{y}_i)\|_2}$ for $(\mathbf{x}_i, \mathbf{y}_i) \in \mathcal{D}$

$i = 1\ N$ Find indices $\{n_j\}_{j=1}^k$ of k nearest neighbors of $\mathbf{x}_i$ from $\mathcal{D} \setminus \{(\mathbf{x}_i, \mathbf{y}_i)\}$ using $d_{\mathcal{X}}$ $*d_{\mathcal{X}}$ can use cached $h_\theta^{\mathcal{X}}$

Find indices $\{m_j\}_{j=1}^k$ of k nearest neighbors of $\mathbf{y}_i$ from $\mathcal{D} \setminus \{(\mathbf{x}_i, \mathbf{y}_i)\}$ using $d_{\mathcal{Y}}$ $*d_{\mathcal{Y}}$ can use cached $h_\theta^{\mathcal{Y}}$

Compute $s_{n,i} := \frac{1}{k} \sum_{j=1}^k d_{\mathcal{Y}}(\mathbf{y}_i, \mathbf{y}_{n_j}) e^{-\tau_{1,n} d_{\mathcal{X}}(\mathbf{x}_i, \mathbf{x}_{n_j})} e^{-\tau_{2,n} d_{mm}(\mathbf{x}_{n_j}, \mathbf{y}_{n_j})}$

Compute $s_{m,i} := \frac{1}{k} \sum_{j=1}^k d_{\mathcal{X}}(\mathbf{x}_i, \mathbf{x}_{m_j}) e^{-\tau_{1,m} d_{\mathcal{Y}}(\mathbf{y}_i, \mathbf{y}_{m_j})} e^{-\tau_{2,m} d_{mm}(\mathbf{x}_{m_j}, \mathbf{y}_{m_j})}$

$s_i := d_{mm}(\mathbf{x}_i, \mathbf{y}_i) + \beta s_{n,i} + \gamma s_{m,i}$

s

To summarize, for each image-caption pair in the dataset, we first compute how similar the image and caption are to each other using a pre-trained CLIP model, which gives a basic measure of how well they match. Then, we compute the nearest neighbors of the caption among other captions in the dataset. For each neighbor, we look at how similar their corresponding image is to the original image. The intuition is that if a sample is correctly labeled, the image should be similar to images of other samples with similar captions. We weight each neighbor based on how close it is to our original sample and how well-matched the neighboring pairs themselves are. Finally, we repeat this for nearest neighbors in the image space. LEMoN is then the weighted sum of these three scores.

D Data Processing

D.1 Classification

We utilize CIFAR10N (`cifar10`) and CIFAR100N (`cifar100`) object detection [82] datasets for all classification-based experiments. Each image is associated with a label indicating the primary object present in the image. These datasets contain 50,000 image-label pairs, with a clean and noisy label available per image. The noisy labels are examples of real human errors within the dataset. Further, we also generate synthetically noised labels as described in the main text. All images are resized to 224x224, center cropped, and normalized using mean and standard deviations corresponding to CLIP during the pre-processing stage. These two datasets are released under the Creative Commons Attribution-NonCommercial 4.0 license.

For `miniImageNet` and `stanfordCars`, we use the "red" datasets from [28], which contain noise from real-world web annotators. We split the full dataset (containing all annotations) into 75%/12.5%/12.5% train/val/test sets, stratifying by the mislabel flag. The annotations are licensed by Google under CC BY 4.0 license, and the images are under CC BY 2.0 license.

D.2 Captioning

We preprocess MSCOCO [42] and Flickr30k [78] by using the Karpathy split [31], and then selecting one random annotation from the ones available. For the MMIMDB dataset [1], we utilize the plot outline as the text, and use the dataset splits provided. For MIMIC-CXR [29], we use all images in the database and the provided data splits, and extract the findings and impression sections from the radiology note for the text modality. Images were normalized and transformed using the same procedure described above.

For downstream captioning, we use the pre-trained tokenizer and image processor corresponding to the pre-trained model (GIT [73]) to pre-process image and captions.

Note that `flickr30k` is available under Flickr terms of use for non-commercial research and/or educational purposes[4]. `mscoco` is available under Creative Commons Attribution 4.0 License. `mmimdb` is available for personal and non-commercial use[5]. Finally, `mimiccxr` is available under the PhysioNet Credentialed Health Data License 1.5.0[6].

[4] `https://shannon.cs.illinois.edu/DenotationGraph/`

[5] `https://developer.imdb.com/non-commercial-datasets/`

[6] `https://physionet.org/content/mimic-cxr/view-license/2.0.0/`

E Baseline Methods

E.1 Classification

Training-dependent

AUM [57]: This model assumes access to a classifier that can predict the class that an image likely belongs to. Then, the margin of difference between the prediction probability from the trained classifier for the assigned class and the class with the (next) highest probability is computed and averaged over training epochs. This score is thresholded to identify potential label errors.

Datamap [67]: Similar to AUM, this method requires access to a pretrained classifier. In this baseline, it is assumed that instances with label errors are 'hard to learn', and thus low confidence in prediction throughout training epochs. To produce a single score, we combine the mean and standard deviation of the probability associated with the assigned class into a single score[7].

Confident Learning [53] is designed to identify labeling errors in classification datasets by modeling the relationship between true class labels and noisy ones. It sets thresholds for each true-noisy label pair. Using these thresholds, the model employs predicted class probabilities to rank predictions for each class, filtering out the noisy data.

Training-free

CLIP Logits [37]: CLIP is used as a zero-shot classifier to obtain the softmax-based probability for the assigned class. This value is then thresholded to identify label errors. Recently, [14] used a similar zero-shot prediction jointly with a semi-supervised training approach for learning in the presence of label noise.

CLIP Similarity [30]: The distance (either euclidean or cosine) between image and text embeddings from CLIP are computed and thresholded.

Deep k-NN[2] The proportion of k nearest neighbors[8] with the same label is computed for each image of interest. Prior works have utilized different representations for obtaining neighbors, including logits and representations from pre-trained [82] vision models. We find that pre-trained representations from CLIP outperformed logits from a zero-shot CLIP classifier [82].

SimiFeat [82] uses nearby features to detect noisy labels under the assumption that local groups of features share clean or noisy labels. **SimiFeat-V** [82] uses local voting and **SimiFeat-R** leverages ranking to detect noisy labels based on HOC estimator. The binary outputs produced are used for all score computations. Note that the difference between Simifeat-V and deep k-NN is in the data processing and augmentation.

Discrepancy [69] finds second-degree nearest neighbors in the text space, then computes the average distance of these neighbors to the original sample in image space. We utilize the same CLIP model to compute semantic distance here as in LEMoN.

E.2 Captioning

Pre-trained or Supervised

LLaVA [44]: We prompt LLaVA (v1.6-vicuna-13b) with the following prompt: `The proposed caption for this image is "{}". Is this caption correct? Only answer with "Yes" or "No".` We examine the probability distribution over the first non-special token, and find the likelihood of the token with the highest probability. If the corresponding token in lower case starts with "yes", we return $1-$ this probability as the mislabel score. Otherwise, we return the probability.

CapFilt (oracle-like): We generate predictions using pre-trained model trained on distinguishing between high-quality MSCOCO and noisy synthetic captions [35]. This forms an oracle-like, fully supervised baseline.

Unsupervised

Datamap: We compute the cross-entropy across training epochs and compute the ratio of the mean and variance in loss across epochs. That is, we expect captioning loss for instances with label errors

[7] We experimented with different strategies, and the square root of the product of the mean and (1-standard deviation) and (1-mean) and standard deviation led to comparable, high validation F1 scores.

[8] Note that this score is not continuous.

to be consistently high. We train captioning models for 3 epochs, with LoRA rank set to 4, and a maximum length of 100[9] for the finetuning task.

Confident Learning: We adapt this approach for dual-modality datasets, such as image-text pairs, by clustering text embeddings to serve as class labels for noise detection.

Downstream-task Unaware

Deep KNN: We cluster captions similar to confident learning, adapting classification baseline.

CLIP Similarity: This is the same setup as classification.

Discrepancy: This is the same setup as classification.

F Compute Setup

We run our experiments on a shared Slurm cluster. Each experiment used one RTX A6000 with 48 GB VRAM, 10 CPU cores of Intel Xeon Ice Lake Platinum 8368, and 50 GB RAM.

G Hyperparameters in Label Error Detection

G.1 Classification

1. AUM, Datamap: learning rate $\in \{5e-5, 5e-6\}$, training for epochs $\in \{5, 10\}$[10]
2. Confident learning: learning rate $\in \{5e-7, 5e-6, 5e-5\}$, upto 30 epochs with early stopping with a patience of 10.
3. CLIP Sim.: cosine distance metric, no other hyperparameters
4. CLIP Zero shot: distance metric
5. Discrepancy: $k \in \{1, 2, 5, 10, 15, 20, 30, 50\}$
6. deep k-NN: k, cosine distance metric

G.2 Captioning

For most baselines requiring a class index–obtained by clustering captions–we set the number of clusters to be 100.

1. LLAVA: Small amount of prompt tuning
2. Confident learning: learning rate $\in \{5e-7, 5e-6, 5e-5\}$, upto 30 epochs, number of clusters
3. CLIP Zero shot: distance metric (either cosine or euclidean)
4. deep k-NN: representation type, $k \in \{1, 2, 5, 10, 15, 20, 30, 50\}$, distance metric (either cosine or euclidean)

G.3 Our Method

We search the following hyperparameters for our $\text{LEMON}_{\text{OPT}}$:

1. $k \in \{1, 2, 5, 10, 15, 20, 30, 50\}$
2. Distance metric (either cosine or euclidean)
3. $\beta, \gamma, \tau_{1,n}, \tau_{2,n}, \tau_{1,m}, \tau_{2,m}$: We take the hyperparameter set which achieves the best validation set F1 from these two strategies: (1) Using Scipy's `minimize` function, with initial guess $(1, 1, ..., 1)$, and with no explicit bounds. (2) Using a grid search with the following grid:
   - $\beta \in \{0, 5, 10, 15, ..., 100\}$
   - $\gamma \in \{0, 5, 10, 15, ..., 100\}$
   - $\tau_{1,n}, \tau_{2,n}, \tau_{1,m}, \tau_{2,m} \in \{0, 1, 5, 10\}$

[9] This is longer than captions in the train sets of all datasets except the medical dataset, and we verified that higher maximum length does not change results.

[10] Note that we experiment with training for fewer epochs to avoid memorization, following [57].

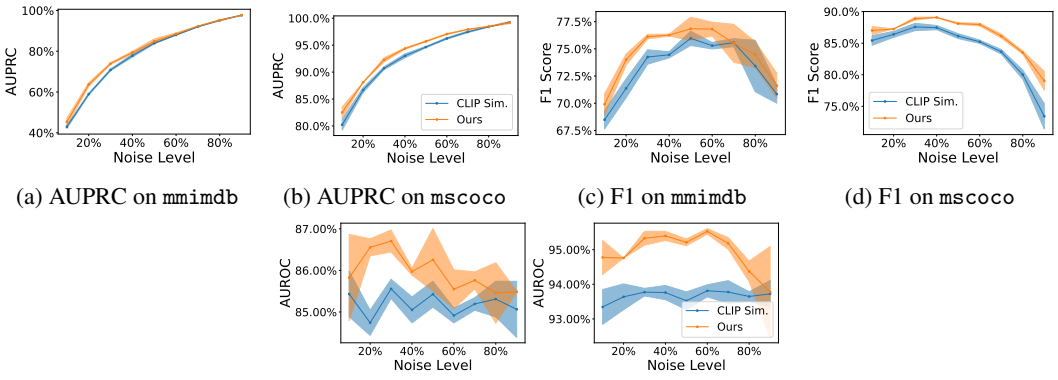

(a) AUPRC on `mmimdb` (b) AUPRC on `mscoco` (c) F1 on `mmimdb` (d) F1 on `mscoco`

(e) AUROC on `mmimdb` (f) AUROC on `mscoco`

Figure I.1: Test-set performance of LEMON$_{\text{OPT}}$ compared to the CLIP similarity baseline for varying levels of the synthetic noise.

H Hyperparameters in Downstream Models

H.1 Classification

We train a Vision Transformer (ViT)-based image classification [13][11] model pre-trained on ImageNet-21k [60] and fine-tuned on ImageNet 2012 [61] with an additional linear layer. We add a linear layer above the classification logits, with an initial learning rate of 0.01, and learning rate scheduling for 10 epochs, and early stopping with a patience of 3. For `miniImageNet`, we use linear probing with just a layer added on top of the standard ViT classification logits (since the pre-trained task matches the downstream task to an extent).

H.2 Captioning

The hyperparameter tuning grid for the captioning model[12] are: learning rate in $\{1e-5, 1e-4\}$, batch size: 16, maximum number of epochs: 10. The model checkpoint from the epoch with lowest validation loss is used for caption generation at test time. For LoRA, we use a rank in {4,16}. For text generation, we use beam search with 4 beams, following [73]. We use the AdamW optimizer [46], with cosine scheduling for learning rate with 1000 warmup steps.

I Additional Experimental Results

I.1 Label Error Detection in Classification Settings

Full results on classification datasets using the noise types bolded in Table 1 (including AUPRC) can be found in Table I.1.

The performance of all baselines and our method on the two types of synthetic errors are shown in Table I.2, all at a noise level of 40% (comparable to the amount of error in the noisy CIFAR datasets).

I.2 Label Error Detection in Captioning Settings

Full results on classification datasets using the noise types bolded in Table 1 (including AUPRC) can be found in Table I.3.

Results on the remaining synthetic noise types (at 40%) can be found in: `flickr30k` I.4, `mscoco` I.5, `mmimdb` I.6, and `mimic-cxr` I.7. Across all datasets and noising types, we find that our model outperforms other non-oracle/supervised baselines.

I.3 Varying Noise Level

We show the AUROC for varying noise levels in Figure I.1.

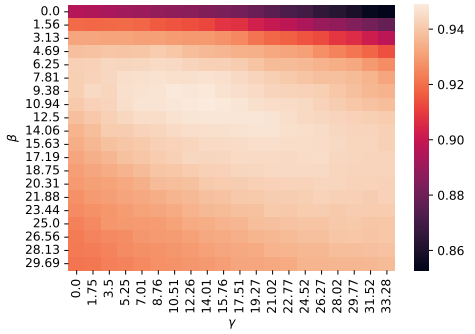

(a) `cifar10`, asymmetric noise

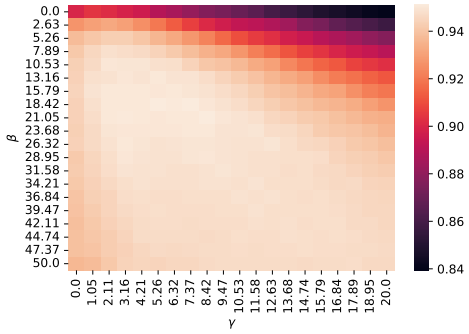

(b) `cifar10`, symmetric noise

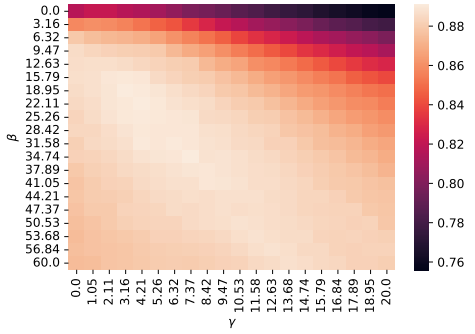

(c) `cifar10`, real noise

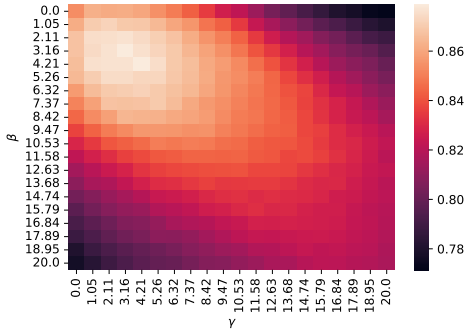

(d) `cifar100`, asymmetric noise

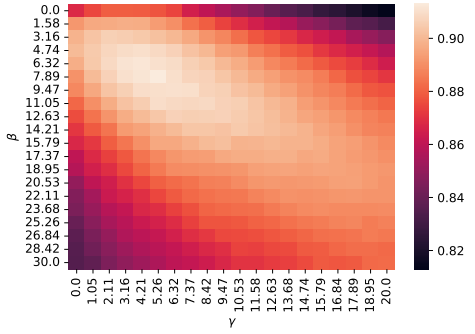

(e) `cifar100`, symmetric noise

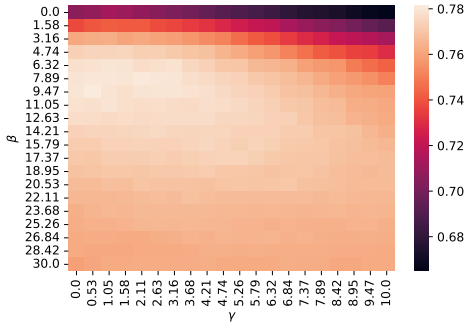

(f) `cifar100`, real noise

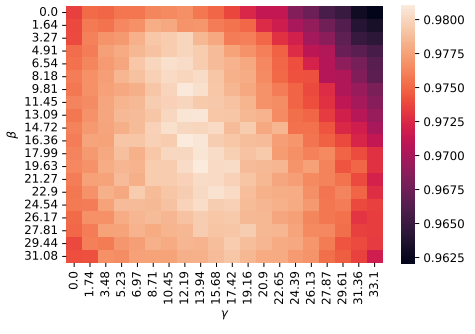

(g) `mscoco`, random noise

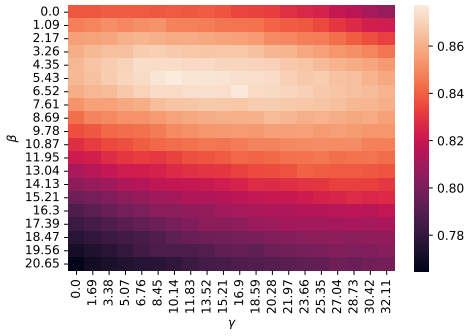

(h) `mscoco`, cat noise

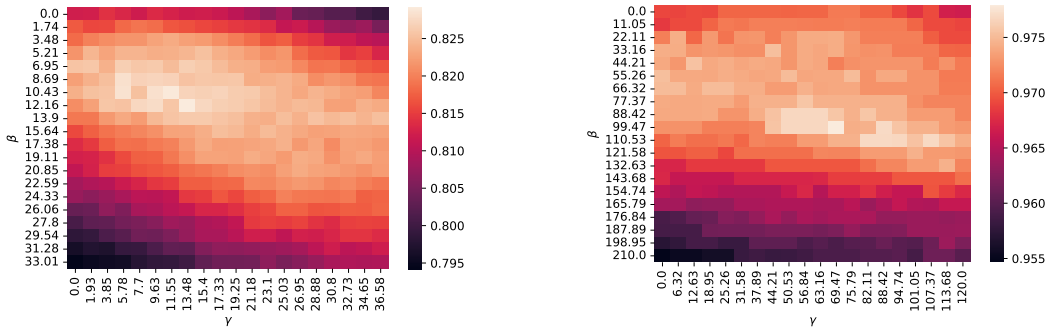

(i) `mscoco`, noun noise

(j) `flickr30k`, random noise

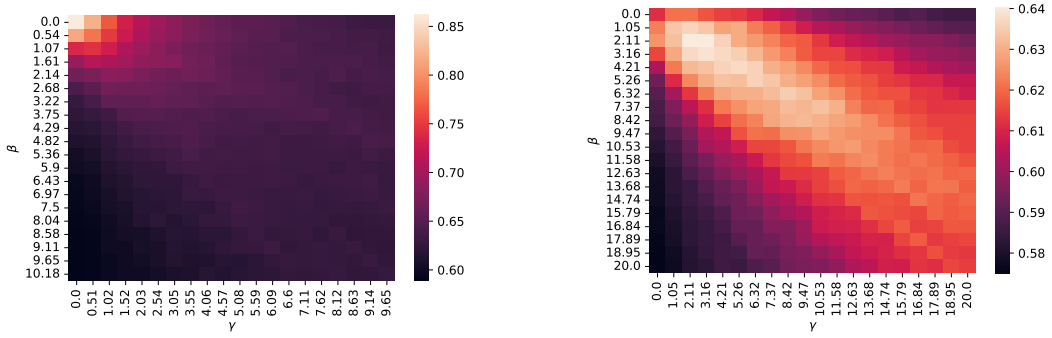

(k) `flickr30k`, noun noise

(l) `mimiccxr`, random noise

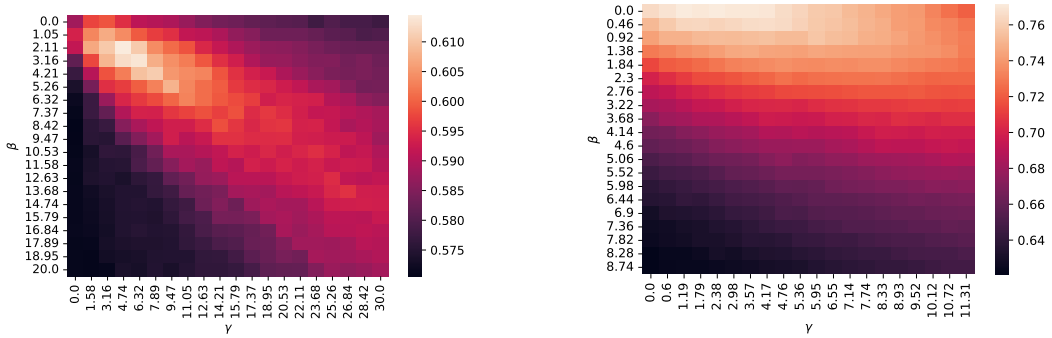

(m) `mimiccxr`, cat noise

(n) `mmimdb`, random noise

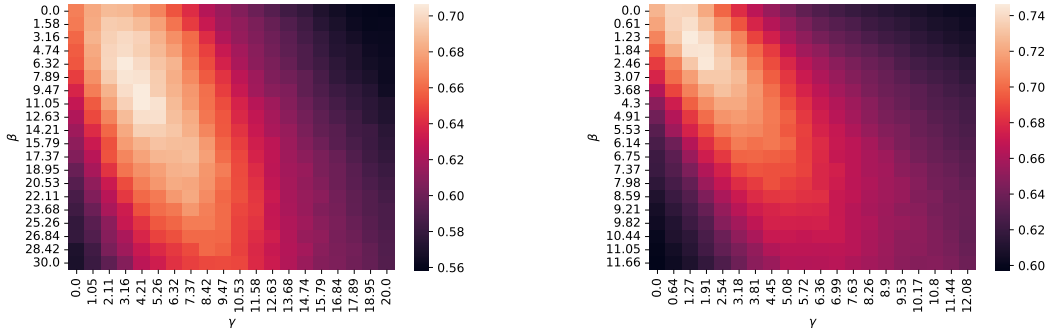

(o) `mmimdb`, noun noise

(p) `mmimdb`, cat noise

Figure I.2: F1 of our method for varying β and γ, keeping all other hyperparameters their fixed optimal values.

Table I.1: Label error detection performance on classification datasets.

Dataset	Method	Training-free	AUROC (%)	AUPRC (%)	F1 (%)
cifar10	AUM	✗	**98.3** (0.1)	**97.9** (0.1)	**94.0** (0.1)
	Datamap		98.2 (0.1)	97.6 (0.1)	93.4 (0.5)
	Confident		93.7 (0.4)	89.4 (0.6)	92.7 (0.5)
	CLIP Logits	✓	95.5 (0.2)	93.9 (0.3)	88.0 (0.5)
	CLIP Sim.		93.8 (0.1)	92.4 (0.2)	86.9 (0.4)
	Simifeat-V		90.6 (0.3)	87.9 (0.7)	88.0 (0.4)
	Simifeat-R		90.7 (0.3)	88.0 (0.4)	88.1 (0.5)
	Discrepancy		77.1 (1.9)	70.4 (2.7)	68.2 (1.9)
	Deep k-NN		97.8 (0.1)	96.5 (0.2)	92.5 (0.5)
	LEMON$_{\text{FIX}}$ (Ours)		97.7 (0.2)	96.8 (0.3)	-
	LEMON$_{\text{OPT}}$ (Ours)		**98.1** (0.0)	**97.4** (0.1)	**93.1** (0.2)
cifar100	AUM	✗	**92.2** (0.2)	**90.0** (0.4)	**83.8** (0.4)
	Datamap		91.8 (0.2)	89.4 (0.3)	83.5 (0.6)
	Confident		74.1 (1.7)	59.3 (2.2)	69.3 (2.0)
	CLIP Logits	✓	84.9 (0.7)	80.3 (1.2)	75.5 (0.5)
	CLIP Sim.		78.5 (0.6)	72.1 (0.7)	69.2 (1.3)
	Simifeat-V		79.5 (0.0)	71.1 (0.8)	73.1 (0.5)
	Simifeat-R		79.7 (0.2)	71.1 (0.8)	73.6 (0.6)
	Discrepancy		66.0 (1.5)	57.4 (2.3)	51.9 (1.8)
	Deep k-NN		87.4 (0.3)	77.9 (1.0)	78.0 (0.3)
	LEMON$_{\text{FIX}}$ (Ours)		88.9 (0.7)	84.6 (1.1)	-
	LEMON$_{\text{OPT}}$ (Ours)		**90.8** (0.0)	**87.4** (0.3)	**81.3** (0.2)
miniImageNet	AUM	✗	83.1 (0.2)	**73.2** (0.5)	75.3 (0.2)
	Datamap		**85.0** (0.2)	71.9 (0.7)	**77.0** (0.2)
	Confident		70.5 (0.2)	52.8 (0.3)	54.7 (0.4)
	CLIP Logits	✓	90.0 (0.2)	80.9 (0.5)	**82.5** (0.2)
	CLIP Sim.		89.3 (0.2)	80.8 (0.3)	81.3 (0.5)
	Simifeat-V		68.2 (0.3)	53.0 (0.4)	55.0 (0.5)
	Simifeat-R		68.0 (0.3)	52.8 (0.3)	54.7 (0.4)
	Discrepancy		79.4 (0.3)	65.6 (0.7)	69.8 (0.4)
	Deep k-NN		83.2 (0.2)	70.9 (0.6)	75.2 (0.4)
	LEMON$_{\text{FIX}}$ (Ours)		89.5 (0.2)	**81.5** (0.3)	-
	LEMON$_{\text{OPT}}$ (Ours)		**90.2** (0.2)	81.4 (1.3)	82.3 (0.1)
stanfordCars	AUM	✗	70.5 (2.4)	**42.8** (1.6)	62.3 (1.2)
	Datamap		**72.3** (1.8)	39.8 (0.5)	**64.9** (2.1)
	Confident		61.0 (0.5)	33.2 (1.7)	43.4 (1.6)
	CLIP Logits	✓	68.8 (0.7)	39.7 (0.9)	64.9 (0.4)
	CLIP Sim.		69.8 (0.6)	40.7 (1.0)	61.7 (0.8)
	Simifeat-V		63.7 (1.2)	33.7 (1.2)	43.7 (1.5)
	Simifeat-R		63.5 (1.3)	33.2 (1.7)	43.4 (1.6)
	Discrepancy		65.7 (0.7)	33.1 (0.6)	59.9 (0.4)
	Deep k-NN		71.4 (0.6)	42.7 (0.5)	65.3 (0.9)
	LEMON$_{\text{FIX}}$ (Ours)		72.6 (0.7)	**44.9** (1.4)	-
	LEMON$_{\text{OPT}}$ (Ours)		**73.1** (0.5)	40.5 (0.5)	**67.3** (1.0)

I.4 Robustness to Hyperparameters

We show the test-set F1 of LEMON for varying β and γ, keeping all other hyperparameters at their fixed optimal values, in Figure I.2. In Table I.8, we show the performance of LEMON when hyperparameters are fixed (at $k = 30$, cosine distance, $\beta = \gamma = 5$, $\tau_{1,n} = \tau_{1,m} = 0.1$, and $\tau_{2,n} = \tau_{2,m} = 5$) versus when they are optimized using a labeled validation set. Note that F1 is not computed as it requires external information to select a threshold.

I.5 Ablations of our Method

Ablations of our method can be found in Table I.9.

[11] `https://huggingface.co/google/vit-base-patch16-224`

[12] `https://huggingface.co/microsoft/git-base`

Table I.2: Label error detection performance on synthetic errors

			AUROC (%)		AUPRC (%)		F1 (%)	
			mean	std	mean	std	mean	std
Dataset	**Flip Type**	**Method**						
cifar10	asymmetric	**AUM**	93.6%	0.6%	86.6%	0.6%	88.9%	0.8%
		Confident	96.2%	0.8%	91.3%	1.6%	95.0%	1.0%
		CLIP Logits	98.8%	0.2%	97.9%	0.3%	94.3%	0.4%
		CLIP Sim.	98.2%	0.2%	97.1%	0.3%	93.4%	0.1%
		Datamap	93.6%	0.5%	86.2%	0.8%	88.2%	0.8%
		Simifeat-V	69.8%	0.5%	58.4%	0.9%	60.4%	0.7%
		Simifeat-R	70.1%	0.5%	58.5%	1.0%	61.1%	0.7%
		Deep k-NN	85.2%	0.7%	66.2%	0.9%	81.1%	1.2%
		LEMON$_{\text{FIX}}$	97.5%	0.2%	94.8%	0.6%	-	-
		LEMON$_{\text{OPT}}$	98.8%	0.2%	97.8%	0.5%	94.9%	0.3%
	symmetric	**AUM**	99.8%	0.0%	99.7%	0.0%	98.4%	0.2%
		Confident	97.6%	0.4%	94.1%	1.3%	96.8%	0.7%
		CLIP Logits	98.5%	0.0%	97.9%	0.1%	93.4%	0.1%
		CLIP Sim.	97.9%	0.0%	97.1%	0.2%	92.5%	0.3%
		Datamap	99.8%	0.0%	99.7%	0.0%	98.3%	0.1%
		Simifeat-V	96.6%	0.0%	94.1%	0.1%	94.3%	0.1%
		Simifeat-R	96.4%	0.2%	93.8%	0.5%	94.1%	0.3%
		Deep k-NN	99.2%	0.1%	98.1%	0.2%	96.7%	0.3%
		LEMON$_{\text{FIX}}$	99.5%	0.1%	99.2%	0.1%	-	-
		LEMON$_{\text{OPT}}$	99.6%	0.1%	99.4%	0.1%	97.3%	0.2%
cifar100	asymmetric	**AUM**	82.4%	2.0%	67.5%	2.6%	75.2%	1.5%
		Confident	63.0%	1.9%	48.4%	1.1%	59.0%	1.5%
		CLIP Logits	96.6%	0.3%	94.8%	0.5%	90.1%	0.7%
		CLIP Sim.	94.7%	0.5%	92.7%	0.7%	87.3%	0.4%
		Datamap	74.0%	1.8%	58.7%	2.3%	65.4%	1.5%
		Simifeat-V	65.5%	1.5%	52.5%	1.8%	57.3%	1.9%
		Simifeat-R	65.3%	1.3%	53.0%	1.6%	56.7%	1.8%
		Deep k-NN	63.3%	0.8%	48.3%	1.1%	55.9%	0.6%
		LEMON$_{\text{FIX}}$	94.9%	0.3%	92.1%	0.4%	-	-
		LEMON$_{\text{OPT}}$	96.6%	0.3%	95.1%	0.2%	90.0%	0.5%
	symmetric	**AUM**	99.2%	0.3%	99.0%	0.5%	96.0%	1.0%
		Confident	88.3%	0.9%	75.3%	1.7%	85.3%	1.2%
		CLIP Logits	96.8%	0.1%	95.2%	0.3%	90.7%	0.4%
		CLIP Sim.	95.1%	0.3%	93.2%	0.5%	87.6%	0.0%
		Datamap	99.2%	0.4%	98.8%	0.7%	95.9%	1.0%
		Simifeat-V	91.2%	0.5%	85.0%	1.2%	84.8%	0.7%
		Simifeat-R	90.9%	0.6%	84.6%	1.2%	84.5%	0.9%
		Deep k-NN	96.7%	0.1%	91.7%	0.3%	92.3%	0.4%
		LEMON$_{\text{FIX}}$	98.4%	0.1%	97.7%	0.2%	-	-
		LEMON$_{\text{OPT}}$	99.0%	0.0%	98.7%	0.1%	95.1%	0.1%

Table I.3: Label error detection performance on captioning datasets.

Dataset	Method	AUROC (%)	AUPRC (%)	F1 (%)
flickr30k	LLaVA	79.3 (0.8)	58.5 (0.2)	65.0 (1.1)
	Datamap	54.0 (1.8)	38.8 (0.6)	28.2 (2.1)
	Discrepancy	73.0 (0.6)	59.2 (1.8)	64.7 (1.7)
	Deep k-NN	71.1 (0.4)	52.0 (1.0)	64.8 (2.7)
	Confident	61.6 (0.5)	40.6 (0.6)	54.3 (0.8)
	CLIP Sim.	**94.8** (0.5)	**92.8** (0.5)	**88.1** (0.7)
	LEMON$_{\text{FIX}}$ (Ours)	93.6 (0.2)	92.0 (0.2)	-
	LEMON$_{\text{OPT}}$ (Ours)	94.5 (0.2)	**92.8** (0.3)	87.7 (0.9)
	CapFilt (Oracle)	98.6 (0.1)	98.1 (0.1)	94.8 (0.5)
mscoco	LLaVA	80.3 (0.1)	63.4 (0.3)	74.9 (0.3)
	Datamap	49.9 (0.7)	40.3 (0.5)	28.6 (0.0)
	Discrepancy	72.7 (0.3)	67.2 (0.4)	67.3 (0.9)
	Deep k-NN	76.6 (0.4)	70.3 (0.6)	73.2 (0.3)
	Confident	66.4 (1.2)	52.1 (1.2)	58.9 (1.5)
	CLIP Sim.	93.8 (0.2)	93.0 (0.4)	87.5 (0.3)
	LEMON$_{\text{FIX}}$ (Ours)	92.0 (0.1)	91.8 (0.3)	-
	LEMON$_{\text{OPT}}$ (Ours)	**95.6** (0.2)	**94.6** (0.3)	**89.3** (0.2)
	CapFilt (Oracle)	99.3 (0.0)	99.1 (0.0)	96.2 (0.3)
mmimdb	LLaVA	58.4 (0.2)	46.4 (0.2)	58.5 (0.1)
	Discrepancy	57.4 (0.4)	45.5 (0.9)	40.2 (1.7)
	Datamap	50.1 (0.5)	40.0 (0.3)	28.9 (0.3)
	deep k-NN	58.7 (0.7)	45.0 (0.5)	44.5 (1.0)
	Confident	52.8 (0.8)	41.4 (0.4)	53.6 (0.7)
	CLIP Sim.	85.1 (0.3)	77.8 (0.7)	74.5 (0.3)
	LEMON$_{\text{FIX}}$ (Ours)	84.3 (0.3)	77.7 (0.8)	-
	LEMON$_{\text{OPT}}$ (Ours)	**86.0** (0.1)	**79.4** (0.6)	**76.3** (0.1)
	CapFilt	82.7 (0.7)	73.3 (1.2)	71.6 (0.8)
mimiccxr	LLaVA	53.9 (0.5)	42.7 (0.7)	28.7 (0.1)
	Datamap	50.2 (0.9)	39.5 (0.9)	28.9 (0.4)
	Discrepancy	60.0 (0.8)	50.3 (0.7)	32.8 (2.8)
	deep k-NN	62.9 (0.4)	48.0 (0.3)	46.0 (4.4)
	Confident	60.2 (0.3)	45.6 (0.3)	59.4 (0.1)
	CLIP Sim.	64.1 (0.4)	51.7 (0.5)	48.6 (3.4)
	LEMON$_{\text{FIX}}$ (Ours)	66.5 (0.2)	54.8 (0.4)	-
	LEMON$_{\text{OPT}}$ (Ours)	**70.4** (2.3)	**60.3** (2.3)	**57.0** (1.6)
	CapFilt	49.2 (0.3)	39.3 (0.6)	28.5 (0.0)

Table I.4: flickr30k: Label Error Detection

Dataset	Noise Type	Method	AUROC		AUPRC		F1	
			mean	std	mean	std	mean	std
flickr30k	noun	**LLAVA**	79.3%	0.8%	58.5%	0.2%	65.0%	1.1%
		captfilt	98.6%	0.1%	98.1%	0.1%	94.8%	0.5%
		Datamap	54.0%	1.8%	38.8%	0.6%	28.2%	2.1%
		Deep kNN	71.1%	0.4%	52.0%	1.0%	64.8%	2.7%
		Confident	61.6%	0.5%	40.6%	0.6%	54.3%	0.8%
		CLIP Sim.	94.8%	0.5%	92.8%	0.5%	88.1%	0.7%
		LEMON$_{\text{FIX}}$	93.6%	0.2%	92.0%	0.2%	-	-
		LEMON$_{\text{OPT}}$	94.5%	0.2%	92.8%	0.3%	87.7%	0.9%
	random	**LLAVA**	81.3%	1.0%	65.6%	1.4%	72.2%	1.1%
		captfilt	99.9%	0.0%	99.8%	0.0%	98.3%	0.2%
		Datamap	50.1%	1.5%	40.6%	1.3%	29.6%	0.9%
		Deep kNN	81.1%	1.6%	65.3%	1.8%	73.0%	1.0%
		Confident	68.5%	1.8%	52.0%	1.5%	66.3%	1.6%
		CLIP Sim.	99.5%	0.1%	99.3%	0.1%	96.4%	0.4%
		LEMON$_{\text{FIX}}$	99.4%	0.2%	99.3%	0.2%	-	-
		LEMON$_{\text{OPT}}$	99.5%	0.2%	99.4%	0.3%	96.9%	0.8%

Table I.5: msccoco: Label Error Detection

Dataset	Noise Type	Method	AUROC		AUPRC		F1	
			mean	std	mean	std	mean	std
mscoco	cat	**LLAVA**	80.3%	0.1%	63.4%	0.3%	74.9%	0.3%
		captfilt	99.3%	0.0%	99.1%	0.0%	96.2%	0.3%
		Datamap	49.9%	0.7%	40.3%	0.5%	28.6%	0.0%
		Deep kNN	76.6%	0.4%	70.3%	0.6%	73.2%	0.3%
		Confident	66.4%	1.2%	52.1%	1.2%	58.9%	1.5%
		CLIP Sim.	93.8%	0.2%	93.0%	0.4%	87.5%	0.3%
		LEMON$_{\text{FIX}}$	92.0%	0.1%	91.8%	0.3%	-	-
		LEMON$_{\text{OPT}}$	95.6%	0.2%	94.6%	0.3%	89.3%	0.2%
	noun	**LLAVA**	79.4%	0.2%	61.3%	0.3%	72.6%	0.2%
		captfilt	98.7%	0.2%	98.4%	0.2%	94.9%	0.4%
		Datamap	51.2%	1.4%	39.4%	1.4%	27.8%	0.4%
		Deep kNN	76.1%	1.3%	68.9%	1.2%	72.3%	1.0%
		Confident	64.6%	1.1%	48.4%	1.1%	55.6%	1.9%
		CLIP Sim.	92.1%	0.2%	90.5%	0.2%	84.8%	0.7%
		LEMON$_{\text{FIX}}$	90.4%	0.5%	89.5%	0.4%	-	-
		LEMON$_{\text{OPT}}$	92.9%	0.5%	91.5%	0.5%	86.1%	0.3%
	random	**LLAVA**	82.6%	0.3%	65.1%	0.6%	76.7%	0.2%
		captfilt	99.9%	0.0%	99.9%	0.0%	99.1%	0.1%
		Datamap	49.9%	0.2%	40.2%	0.3%	28.6%	0.0%
		Deep kNN	93.8%	0.2%	85.8%	0.3%	89.2%	0.5%
		Confident	83.5%	1.5%	69.4%	2.3%	80.2%	1.6%
		CLIP Sim.	99.5%	0.1%	99.4%	0.1%	97.6%	0.1%
		LEMON$_{\text{FIX}}$	99.5%	0.2%	99.4%	0.1%	-	-
		LEMON$_{\text{OPT}}$	99.6%	0.1%	99.5%	0.1%	97.9%	0.1%

Table I.6: mmimdb: Label Error Detection

Dataset	Noise Type	Method	AUROC		AUPRC		F1	
			mean	std	mean	std	mean	std
mmimdb	cat	**LLAVA**	58.4%	0.2%	46.4%	0.2%	58.5%	0.1%
		captfilt	82.7%	0.7%	73.3%	1.2%	71.6%	0.8%
		Datamap	50.1%	0.5%	40.0%	0.3%	28.9%	0.3%
		Deep kNN	58.7%	0.7%	45.0%	0.5%	44.5%	1.0%
		Confident	52.8%	0.8%	41.4%	0.4%	53.6%	0.7%
		CLIP Sim.	85.1%	0.3%	77.8%	0.7%	74.5%	0.3%
		LEMON$_{\text{FIX}}$	84.3%	0.3%	77.7%	0.8%	-	-
		LEMON$_{\text{OPT}}$	86.0%	0.1%	79.4%	0.6%	76.3%	0.1%
	noun	**LLAVA**	59.1%	0.3%	44.2%	0.6%	55.2%	0.2%
		captfilt	79.9%	0.1%	66.2%	0.4%	70.0%	0.3%
		Datamap	50.3%	0.4%	37.2%	0.7%	28.0%	1.5%
		Deep kNN	61.4%	0.1%	44.2%	0.3%	45.3%	4.1%
		Confident	52.1%	2.2%	38.0%	1.3%	50.3%	1.6%
		CLIP Sim.	82.8%	0.4%	72.8%	0.5%	72.7%	0.4%
		LEMON$_{\text{FIX}}$	82.1%	0.4%	72.7%	0.6%	-	-
		LEMON$_{\text{OPT}}$	84.4%	0.2%	75.9%	1.2%	75.2%	0.1%
	random	**LLAVA**	58.5%	0.8%	46.7%	0.5%	58.5%	0.1%
		captfilt	84.9%	0.4%	76.4%	0.7%	73.6%	0.2%
		Datamap	50.6%	0.2%	40.4%	0.4%	29.3%	0.6%
		Deep kNN	62.1%	0.5%	47.3%	0.3%	50.0%	0.6%
		Confident	52.9%	1.8%	41.5%	0.9%	54.1%	2.1%
		CLIP Sim.	88.1%	0.1%	82.0%	0.2%	78.2%	0.9%
		LEMON$_{\text{FIX}}$	87.6%	0.1%	81.9%	0.3%	-	-
		LEMON$_{\text{OPT}}$	89.4%	0.3%	84.1%	0.8%	80.1%	0.4%

Table I.7: mimiccxr: Label Error Detection

Dataset	Noise Type	Method	AUROC		AUPRC		F1	
			mean	std	mean	std	mean	std
mimiccxr	cat	**LLAVA**	53.9%	0.5%	42.7%	0.7%	28.7%	0.1%
		captfilt	49.2%	0.3%	39.3%	0.6%	28.5%	0.0%
		Datamap	50.2%	0.9%	39.5%	0.9%	28.9%	0.4%
		Deep kNN	62.9%	0.4%	48.0%	0.3%	46.0%	4.4%
		Confident	60.2%	0.3%	45.6%	0.3%	59.4%	0.1%
		CLIP Sim.	64.1%	0.4%	51.7%	0.5%	48.6%	3.4%
		LEMoN$_{\text{FIX}}$	66.6%	0.2%	54.8%	0.4%	-	-
		LEMoN$_{\text{OPT}}$	70.4%	2.3%	60.3%	2.3%	57.0%	1.6%
	random	**LLAVA**	50.8%	0.4%	40.6%	0.2%	57.1%	0.0%
		captfilt	50.8%	0.4%	40.5%	0.7%	28.6%	0.0%
		Datamap	51.1%	0.9%	40.7%	0.5%	28.8%	0.2%
		Confident	61.1%	0.7%	46.3%	0.5%	60.7%	0.5%
		CLIP Sim.	66.8%	0.8%	54.4%	0.9%	54.3%	1.0%
		LEMoN$_{\text{FIX}}$	69.5%	0.7%	57.8%	1.0%	-	-
		LEMoN$_{\text{OPT}}$	73.1%	0.9%	63.0%	2.0%	63.1%	3.6%

Table I.8: We show the AUROC and AUPRC of LEMoN when we search for the optimal hyperparameters using a labeled validation set (LEMoN$_{\text{OPT}}$) and when we use fixed hyperparameters (LEMoN$_{\text{FIX}}$: $k = 30$, cosine distance, $\beta = \gamma = 5$, $\tau_{1,n} = \tau_{1,m} = 0.1$, and $\tau_{2,n} = \tau_{2,m} = 5$). The mean gap in AUROC is -1.6 (1.3), and the mean gap in AUPRC is -1.6 (2.2). Note that F1 is not computed as it requires external information to select a threshold.

		AUROC			AUPRC		
Dataset	**Noise Type**	**LEMoN$_{\text{OPT}}$**	**LEMoN$_{\text{FIX}}$**	**Gap**	**LEMoN$_{\text{OPT}}$**	**LEMoN$_{\text{FIX}}$**	**Gap**
cifar10	**asymmetric**	98.8 (0.2)	97.5 (0.2)	-1.4 (0.1)	97.8 (0.5)	94.8 (0.6)	-3.0 (0.1)
	real	98.1 (0.0)	97.7 (0.2)	-0.5 (0.2)	97.4 (0.1)	96.8 (0.3)	-0.5 (0.2)
	symmetric	99.6 (0.1)	99.5 (0.1)	-0.2 (0.1)	99.4 (0.1)	99.2 (0.1)	-0.2 (0.1)
cifar100	**asymmetric**	96.6 (0.3)	94.9 (0.3)	-1.8 (0.0)	95.1 (0.2)	92.1 (0.4)	-3.0 (0.2)
	real	90.8 (0.0)	88.9 (0.7)	-1.8 (0.7)	87.4 (0.3)	84.6 (1.1)	-2.8 (0.9)
	symmetric	99.0 (0.0)	98.4 (0.1)	-0.7 (0.1)	98.7 (0.1)	97.7 (0.2)	-1.0 (0.1)
miniImageNet	**human**	90.2 (0.2)	89.5 (0.2)	-0.7 (0.2)	81.4 (1.3)	81.5 (0.3)	0.0 (0.1)
StanfordCars	**human**	73.1 (0.5)	72.6 (0.7)	-0.7 (0.1)	40.5 (0.5)	44.9 (1.4)	4.3 (0.7)
flickr30k	**noun**	94.5 (0.2)	93.6 (0.2)	-0.9 (0.3)	92.8 (0.3)	92.0 (0.2)	-0.8 (0.1)
	random	99.5 (0.2)	99.4 (0.2)	-0.0 (0.1)	99.4 (0.3)	99.3 (0.2)	-0.1 (0.2)
mimiccxr	**cat**	70.4 (2.3)	66.5 (0.2)	-3.9 (2.1)	60.3 (2.3)	54.8 (0.4)	-5.5 (1.9)
	random	73.1 (0.9)	69.5 (0.7)	-3.6 (0.2)	63.0 (2.0)	57.8 (1.0)	-5.1 (1.0)
mmimdb	**cat**	86.0 (0.1)	84.3 (0.3)	-1.6 (0.3)	79.4 (0.6)	77.7 (0.8)	-1.7 (0.2)
	noun	84.4 (0.2)	82.1 (0.4)	-2.3 (0.3)	75.9 (1.2)	72.7 (0.6)	-3.2 (0.8)
	random	89.4 (0.3)	87.6 (0.1)	-1.8 (0.4)	84.1 (0.8)	81.9 (0.3)	-2.2 (0.8)
mscoco	**cat**	95.6 (0.2)	92.0 (0.1)	-3.6 (0.1)	94.6 (0.3)	91.8 (0.3)	-2.8 (0.1)
	noun	92.9 (0.5)	90.4 (0.5)	-2.5 (0.2)	91.5 (0.5)	89.5 (0.4)	-2.0 (0.3)
	random	99.6 (0.1)	99.5 (0.2)	-0.1 (0.0)	99.5 (0.1)	99.4 (0.1)	-0.1 (0.0)

Table I.9: Performance of our method after ablating various components. We find that mislabel detection performance almost decreases monotonically as we remove additional components, with the exception of two metrics on mmimdb where one ablation is statistically comparable to the original method.

	mmimdb			mscoco		
	AUROC	**AUPRC**	**F1**	**AUROC**	**AUPRC**	**F1**
LEMoN$_{\text{OPT}}$ (Ours)	86.0 (0.1)	79.4 (0.6)	**76.3** (0.1)	**95.5** (0.1)	**94.5** (0.3)	**89.3** (0.3)
$-\tau_1$	85.3 (0.3)	78.2 (1.1)	75.4 (0.5)	94.6 (0.3)	93.8 (0.4)	88.0 (0.5)
$-\tau_2$	85.4 (0.6)	77.1 (2.4)	75.4 (0.2)	94.7 (0.3)	93.6 (0.5)	87.7 (0.8)
$-\tau_1, \tau_2$	85.4 (0.2)	78.1 (0.7)	75.2 (0.3)	94.7 (0.3)	93.8 (0.5)	88.0 (0.8)
$-s_n$	**86.1** (0.3)	**79.6** (0.5)	76.1 (1.1)	94.6 (0.3)	93.6 (0.5)	87.5 (0.6)
$-s_m$	85.3 (0.3)	77.9 (0.7)	75.5 (0.4)	94.9 (0.2)	94.0 (0.4)	89.0 (0.6)
$-s_n, s_m$ (CLIP Sim.)	85.1 (0.3)	77.8 (0.7)	74.5 (0.3)	93.8 (0.2)	93.0 (0.4)	87.5 (0.3)

I.6 Varying Validation Set Size

In Figure I.3, we examine the effect of varying validation set size (by random subsampling) on LEMON$_{\text{OPT}}$.

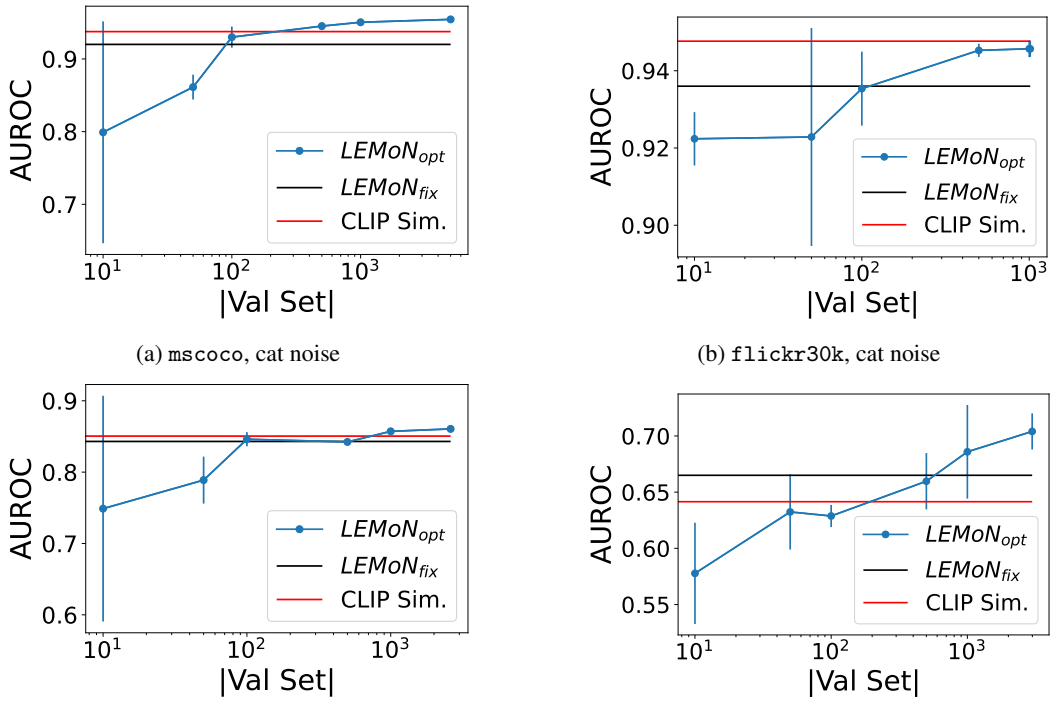

(a) `mscoco`, cat noise

(b) `flickr30k`, cat noise

(c) `mmimdb`, noun noise

(d) `mimiccxr`, cat noise

Figure I.3: Test-set AUROC of mislabel detection with varying size of the labeled validation set for LEMON$_{\text{OPT}}$. Note that LEMON$_{\text{FIX}}$ and CLIP Sim. do not have any hyperparameters and as such do not rely on a labeled validation set.

I.7 Empirical Comparison with [69]

In Table I.10, we compare the performance of LEMON$_{\text{OPT}}$ against the four scores proposed in [69], using the datasets and noise types shown in Table 1.

Table I.10: Comparison of label error detection performance of LEMoN versus baselines from [69].

	AUROC					AUPRC					F1				
	Υ_X^{DIS}	Υ_Y^{DIS}	Υ_X^{DIV}	Υ_Y^{DIV}	LEMON$_{\text{OPT}}$	Υ_X^{DIS}	Υ_Y^{DIS}	Υ_X^{DIV}	Υ_Y^{DIV}	LEMON$_{\text{OPT}}$	Υ_X^{DIS}	Υ_Y^{DIS}	Υ_X^{DIV}	Υ_Y^{DIV}	LEMON$_{\text{OPT}}$
`cifar10`	77.1 (1.9)	48.2 (1.2)	50.3 (1.9)	45.0 (1.9)	**98.1** (0.0)	70.4 (2.7)	41.2 (1.1)	41.6 (1.6)	38.9 (2.1)	**97.4** (0.1)	68.2 (1.9)	29.2 (0.4)	29.2 (0.4)	29.2 (0.4)	**93.1** (0.2)
`cifar100`	66.0 (1.5)	49.4 (1.1)	49.9 (1.4)	49.7 (1.9)	**90.8** (0.0)	57.4 (2.3)	39.2 (0.7)	39.9 (1.2)	39.3 (0.8)	**87.4** (0.3)	51.9 (1.8)	29.4 (1.4)	32.5 (5.5)	29.4 (0.4)	**81.3** (0.2)
`miniImageNet`	79.4 (0.3)	47.4 (0.5)	64.6 (0.2)	48.0 (0.5)	**90.2** (0.2)	65.6 (0.7)	32.5 (0.0)	46.3 (0.2)	32.7 (0.8)	**81.4** (1.3)	69.8 (0.4)	28.0 (2.3)	55.8 (2.3)	27.0 (0.9)	**82.3** (0.1)
`stanfordCars`	65.7 (0.7)	50.8 (1.1)	51.9 (0.9)	50.1 (0.5)	**73.1** (0.5)	33.1 (0.6)	23.3 (0.7)	24.5 (0.8)	23.4 (0.2)	**40.5** (0.5)	59.9 (0.4)	20.6 (1.3)	25.3 (5.6)	20.6 (1.4)	**67.3** (1.0)
`flickr30k`	73.0 (0.6)	53.3 (1.4)	49.9 (2.9)	52.9 (0.2)	**94.5** (0.2)	59.2 (1.8)	37.1 (1.8)	33.7 (2.4)	37.0 (0.8)	**92.8** (0.3)	64.7 (1.7)	26.2 (0.8)	27.4 (1.7)	26.1 (1.0)	**87.7** (0.9)
`mimiccxr`	60.0 (0.8)	49.6 (0.4)	50.0 (1.3)	49.1 (1.3)	**70.4** (2.3)	50.3 (0.7)	39.3 (0.5)	39.8 (1.2)	39.6 (0.7)	**60.3** (2.3)	32.8 (2.8)	28.5 (0.0)	28.5 (0.0)	28.5 (0.0)	**57.0** (1.6)
`mmimdb`	57.4 (0.4)	49.8 (0.4)	48.6 (0.4)	50.0 (0.5)	**86.0** (0.1)	45.5 (0.9)	40.1 (0.4)	38.9 (0.5)	40.1 (0.5)	**79.4** (0.6)	40.2 (1.7)	28.6 (0.1)	29.1 (0.5)	28.9 (0.6)	**76.3** (0.1)
`mscoco`	72.7 (0.3)	48.5 (0.8)	52.9 (0.8)	48.7 (0.3)	**95.6** (0.2)	67.2 (0.4)	39.1 (0.5)	42.3 (1.0)	39.3 (0.1)	**94.6** (0.3)	67.3 (0.9)	29.7 (0.1)	29.0 (0.2)	28.9 (0.4)	**89.3** (0.2)

I.8 Real-World Web Scale Corpus

We conduct an experiment of LEMON$_{\text{FIX}}$ on CC3M [7], a large web-scraped dataset of images and annotations, where we demonstrate the utility of LEMON filtered data on CLIP pretraining. We download CC3M, which contains 2.9 million valid URLs to image-caption pairs. We then pretrain a CLIP model (ViT-B/16) from scratch on this dataset for 20 epochs, with a batch size of 128, and using a cyclic learning rate scheduler with a learning rate of 10^{-4}.

We then use this CLIP model as the basis to compute distances for LEMON$_{\text{FIX}}$, using the reasonable hyperparameters from the main paper: $k = 30$, cosine distance, $\tau_{1,n} = \tau_{1,m} = 0.1$, and $\tau_{2,n} = \tau_{2,m} = 5$. We then select the 1 million samples with the lowest mislabel scores, filtering out the 1.9 million samples most suspected to be mislabels. We pre-train another CLIP model from scratch on this subset using the same architecture and setup as above. We evaluate the resulting model on zero-shot classification using the VTAB benchmark [79], and compare it with CLIP models trained

using data filtered to 1 million examples using the CLIP similarity baseline, and the original unfiltered model.

In Table I.8, we find that LEMON$_{\text{FIX}}$ marginally outperforms the CLIP similarity baseline on average zero-shot accuracy, though both underperform pretraining on the full corpus. One likely explanation of this is that although a large proportion of images in the CC3M dataset are technically "mislabelled" in that the caption is not a precisely correct description of the image, some substrings of these noisy captions may, on aggregate, contain useful word associations which the model learns, and thus may be useful to downstream tasks.

We examine images of images selected to be mislabels by our method in Figure I.4. We find that our method identifies images that are completely mislabeled – one cause of which is images changing after they have been indexed. In addition, our method also identifies samples which are ambiguous or imprecise.

Table I.11: Zero-shot accuracy (%) of various CLIP models on the VTAB benchmark [79]. CLIP models (ViT-B/16) are pretrained from scratch on a subset of CC3M [7] which has been filtered to 1 million samples using LEMON$_{\text{FIX}}$ and the CLIP similarity baseline, using a version of CLIP pretrained on the entire dataset.

	CLIP Sim.	**LEMON$_{\text{FIX}}$**	**Unfiltered**
caltech101	28.25	**28.99**	51.43
cifar100	**11.02**	6.79	18.65
clevr_closest_object_distance	18.11	**22.58**	25.76
clevr_count_all	**12.98**	12.65	12.05
dmlab	14.78	**16.22**	16.62
dsprites_label_orientation	**2.44**	1.34	1.98
dsprites_label_x_position	3.06	**3.20**	3.13
dsprites_label_y_position	**3.11**	2.89	3.20
dtd	**6.60**	3.94	12.34
eurosat	14.37	**22.07**	9.93
flowers	**6.11**	5.19	6.83
food101	4.94	**5.31**	9.02
pets	**7.63**	4.69	8.23
sun397	13.89	**14.22**	24.02
svhn	7.80	**12.35**	8.00
Average	10.34	**10.83**	14.08

I.9 Hyperparameters Used for Real-World

We show the hyperparameters used for the real-world experiment in Table I.12. We use $k = 30$, cosine distance, and these hyperparameters, which originate from a hyperparameter search on synthetically noised data. We note that `flickr30k` has some negative hyperparameters, which we attribute to overfitting to a relatively small validation set during hyperparameter selection.

Table I.12: Hyperparameters used for the real-world experiment. We use $k = 30$, cosine distance, and the hyperparameters below, which originate from a hyperparameter search on synthetically noised data.

	β	γ	$\tau_{1,n}$	$\tau_{2,n}$	$\tau_{1,m}$	$\tau_{2,m}$
`cifar10`	20	10	0	5	0	5
`cifar100`	15	0	0	5	0	0
`mscoco`	5.324	11.057	5.143	10.498	7.233	15.637
`mmimdb`	15	5	5	10	5	10
`flickr30k`	0.092	-0.177	-0.274	-0.074	-0.072	0.000
`mimiccxr`	5	10	5	10	5	10

I.10 Examples of Detected Real Label Errors

We show additional examples of label errors in Figure I.5.

fresh milk in the glass on colour background, illustration

a very young baby girl playing with toys in a white studio

portrait of a stock photo

homes for sale and luxury real estate including horse farms and property in the areas

tangled tree roots on a forest trail

a park covered in yellow leaves and lined with tall trees turning bright yellow during an autumn day

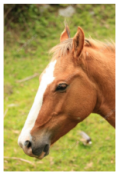

face of people -- stock photo #

begin your exercise with a jump rope easy and funny

evil looking person sitting atop a hay bale royalty - free

Figure I.4: Sample images and captions from CC3M which have been identified as mislabeled by LEMON$_{\text{FIX}}$.

Figure I.5: Example images in each dataset identified by our method to be mislabels, and labeled as errors by a human annotator.

I.11 Comparison with Northcutt et al., 2021 [54]

In Northcutt et al., 2021 [54], the authors utilized confident learning [53] to identify suspected errors in the test sets of `cifar10` and `cifar100`. They then obtained 5 human labels for each suspected error using Amazon Mechanical Turk, and confirmed the image to be a mislabel if at least 3 of 5 workers stated so. This amounts to 54 confirmed mislabels in `cifar10` (out of 221 suspected), and 585 confirmed mislabels in `cifar100` (out of 1650 suspected). In this section, we compare the performance of LEMON$_{\text{FIX}}$ versus the CLIP similarity baseline on this set. As this set is a subset of the images identified to be mislabels by confident learning, we are not able to compare our model performance with confident learning itself. In addition, this presents a pessimistic view (lower bound) of the performance of our method, as there are many images identified by LEMON which *are* mislabeled, but were not selected by confident learning in [54]. We demonstrate examples of these images in Figure I.6.

In Table I.13, we compare the performance of LEMON$_{\text{FIX}}$ with the CLIP similarity baseline on the error set from Northcutt et al., 2021 [54]. First, we compute the mean ranking of all error set samples as ranked by each method, out of 10,000 test-set samples. We find that our method ranks error set samples higher on average than the baseline, though the variance is large. Next, we subset to the top |CL Set| ranked samples for each method, and compute the percentage of which are actually in the error set. We note that this precision metric is upper bounded by the precision of the reference method (confident learning). Again, we find that LEMON$_{\text{FIX}}$ outperforms the baseline, and is able to identify more actual label errors than CLIP similarity at this threshold.

Figure I.6: Demonstrative examples of mislabeled samples in `cifar10` and `cifar100` which have been identified by our method in the top |CL Set|, but was not identified by confident learning in Northcutt et al., 2021 [54] and thus was not a part of their error set.

Table I.13: Comparison of LEMON$_{\text{FIX}}$ (Ours) with the CLIP similarity baseline on the human labeled error set from Northcutt et al., 2021 [54]. In this prior work, the authors used confident learning to identify |CL Set| candidate label errors in `cifar10` and `cifar100`, |Error Set| of which are confirmed to be mislabels by Mechanical Turkers. Mean Ranking denotes the average ranking of all error set samples as ranked by each method. Precision @ Top |CL Set| involves taking the top |CL Set| samples as ranked by each method, and computing the percentage of which are in the error set. Note that each dataset's test set consists of 10,000 samples. Numbers in parentheses represent one standard deviation.

			Mean Ranking		**Precision @ Top |CL Set|**		
Dataset	**|CL Set|**	**|Error Set|**	**LEMON$_{\text{FIX}}$**	**CLIP Sim.**	**Oracle**	**LEMON$_{\text{FIX}}$**	**CLIP Sim.**
`cifar10`	275	54	1269.7 (1905.1)	2681.0 (2507.1)	19.64%	6.55%	1.45%
`cifar100`	2235	585	2357.5 (1981.5)	3642.1 (2719.5)	26.17%	14.41%	10.16%

Table I.14: We manually label 200 images from real-world datasets that each method identifies as the most likely to be mislabeled and show the percentage (%) of times where it is actually mislabeled. Numbers in parentheses are 95% confidence intervals from a binomial proportion.

	CLIP Sim.	Ours
cifar10	5.5 (3.2)	**10.0** (4.2)
cifar100	11.0 (4.3)	**20.5** (5.6)
flickr30k	32.5 (6.5)	**41.0** (6.8)
mscoco	19.5 (5.5)	**25.5** (6.0)

I.12 Downstream Classification with Label Error Detection-based Filtering

Here, we show the impact of filtering out different proportions of the training data based on label error predictions, and obtaining test performance.

I.12.1 Average accuracy

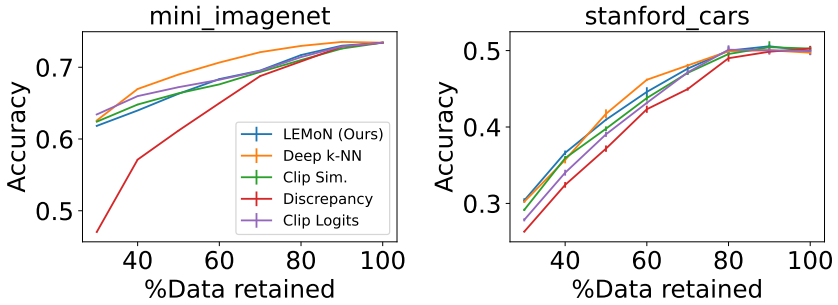

Figure I.7: Downstream accuracy on `stanfordCars`, and `miniImageNet`.

I.13 Out-of-Domain Robustness

We report the test performance on an Out-of-Domain (OOD) dataset CIFAR-10C [22], when models are trained on the `cifar10` noisy train set, and validated and tested with clean data with early stopping. The CIFAR-10C dataset contains 19 corruptions applied to the `cifar10` test set, with varying severity of corruption. Then, robustness is measured as the average test top-1 class accuracy performance on the CIFAR-10C dataset (across all corruption types and severities), following prior work [12]. We see that: highest robustness is obtained when the proportion of data retained in the train set = 60%, which matches the degree of noise in the dataset. Thus, this implies that filtering out atypical samples using LEMoN increases robustness to image corruptions.

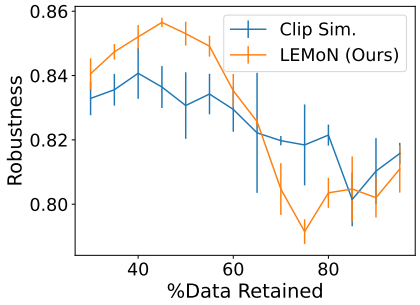

Figure I.8: Downstream accuracy on CIFAR-10C, averaged across all corruption types.